UNIVERSITÄT LEIPZIG
FAKULTÄT FÜR BIOWISSENSCHAFTEN;
PHARMAZIE UND PSYCHOLOGIE
Institut für Biologie

Activation of dendritic cells and keratinocytes by *Parapoxvirus ovis*

Abschlussarbeit zur Erlangung des akademischen Grades
Master of Science (M. Sc.)

vorgelegt von

Susann Hähnel

geb. am 10.11.1990 in Schkeuditz

Gutachter: *Prof. Dr. Thomas M. Magin*
Gutachter: *Prof. Dr. Gottfried Alber*

Erklärung

Ich versichere hiermit, dass ich die vorliegende Arbeit selbstständig verfasst und keine anderen als die im Literaturverzeichnis angegebenen Quellen benutzt habe.

Alle Stellen, die wörtlich oder sinngemäß aus veröffentlichten oder noch nicht veröffentlichten Quellen entnommen sind, sind als solche kenntlich gemacht.

Die Zeichnungen oder Abbildungen in dieser Arbeit sind von mir selbst erstellt worden oder mit einem entsprechenden Quellennachweis versehen.

Diese Arbeit ist in gleicher oder ähnlicher Form noch bei keiner anderen Prüfungsbehörde eingereicht worden.

Leipzig, den 18.07.2014

List of abbreviations

7-AAD	7-aminoactinomycin D
A	area
APC	allophycocyanin
BSA	bovine serumalbumin
CD	cluster of differentiation
cDC	conventional dendritic cells
CpG-ODN	cytosine-phosphate-guanine-oligodesoxynucleotides
Cy2	cyanine
DC	dendritic cells
DMSO	dimethyl sulfoxide
EDTA	ethylenediaminetetraacetic acid
e.g.	*exempli gratia*
EGF	epidermal growth factor
FBS	foetal bovine serum
FITC	fluorescein isothiocyanate
FLDC	Flt3L-derived dendritic cells
Flt3L	fms-like tyrosine kinase 3-ligand
FSC	forward scatter
g	gravitational acceleration
ICAM-1	intercellular adhesion molecule 1
i.e.	*id est*
IF	immunofluorescence
IFN	interferon
IgG	immunoglobulin G
IL	interleukin
iPPVO	(chemically) inactivated *Parapoxvirus ovis*
LC	Langerhans cells
LD dye	Fixable Viability Dye eFluor® 780 (“Life Death dye”)
MHC-I	major histocompatibility complex I
MHC-II	major histocompatibility complex II
MOI	multiplicity of infection
PBS	phosphate buffered saline
pDC	plasmacytoid dendritic cells

PD-L1	programmed death-ligand 1
PE	phycoerythrin
PerCP	peridinin chlorophyll
PPVO	*Parapoxvirus ovis*
PRR	pattern recognition receptors
P/S	penicillin/streptomycin
RPMI	Roswell Park Memorial Institute
SSC	sideward scatter
TLR	toll-like receptor
TMB	tetramethylbenzidine
TNF-α	tumor necrosis factor α
TSLP	thymic stromal lymphopoietin
VACV	Vaccinia virus
vPPVO	replication-competent (“viable”) *Parapoxvirus ovis*
W	width

Summary

Parapoxvirus ovis (PPVO) causes orf (contagious ecthyma, scabby mouth, contagious pustular dermatitis) – a debilitating skin disease mainly infecting sheep and goats. Also humans with direct contact to diseased animals can be infected.

Dendritic cells (DC) as professional antigen-presenting cells are among the first cells to get in contact with invading pathogens. Thus, the investigation of the interaction of PPVO and DC is of great interest.

PPVO is an epitheliotropic virus causing localized skin lesions. In sheep, it is reported that keratinocytes are target cells of PPVO replication. During this study it was investigated how cultured murine keratinocytes, originally isolated from the epidermis of newborn mice and selected for spontaneously immortalized cells in culture, respond to infection with PPVO, especially in comparison to DC, *in vitro* generated from bone marrow.

Upon PPVO infection, DC produced IL-6, IL-12p40, TNF-α and type I and III interferons, demonstrating an activation state of these cells. In contrast to DC, keratinocytes upregulated only IL-1β secretion in response to PPVO and showed no production of IL-6, IL-12p40 and interferons.

Furthermore, DC upregulated the expression of the antigen-presenting molecule MHC-II as well as the co-stimulatory molecule CD86 following PPVO stimulation. Keratinocytes were analyzed regarding the expression of MHC-I, MHC-II, ICAM-1 and PD-L1 in response to PPVO. It was observed that keratinocytes do not upregulate any of the investigated surface molecules. In summary, fundamental differences concerning the activation by PPVO were observed between murine DC and keratinocytes – PPVO preferentially activates DC rather than keratinocytes.

To explain the observed differences in response to PPVO infection, I analyzed differences in cytotoxicity and uptake of PPVO into the cells. Staining of infected cells with annexin-V and 7-AAD revealed that the viability of conventional DC (cDC) is severely reduced upon PPVO infection whereas the viability of plasmacytoid DC (pDC) and keratinocytes was not affected. These data indicate that cDC are more susceptible to PPVO than keratinocytes and pDC. Thus, the different activation properties of DC and keratinocytes cannot be explained by cytotoxicity. Apoptosis was not induced in keratinocytes by PPVO. For apoptosis analysis in DC, further studies are necessary.

The second approach to explain the different responses of both cell types to PPVO infection, was to analyze the magnitude of the uptake of the virus into the cells. DC and keratinocytes

were both able to take up PPVO, but the frequency of infected cells was higher in DC. However, keratinocytes showed a higher PPVO per cell uptake than DC.

The reasons for the distinct responses of keratinocytes and DC to PPVO infection cannot be explained by cytotoxicity or differences in viral uptake. Future studies will be done to clarify the intracellular localization of PPVO in pDC, cDC and keratinocytes. Differences in the intracellular distribution of PPVO could indicate distinct infection pathways in both cell types resulting in distinct signal transduction cascades, and thus provide the explanation for the differences in the virus-induced activation properties.

Contents

Erklärung 2
List of abbreviations 3
Summary 5
Contents 7
List of figures 9
List of tables 10
1. Introduction 11
1.1 *Parapoxvirus ovis* and the innate immune system 11
1.2 Dendritic cells in anti-viral immunity 12
1.3 Keratinocytes as target cells for PPVO infection 13
1.4 Aim of the study 14
2. Materials 15
2.1 Mice 15
2.2 Cells 15
2.2.1 Murine keratinocytes 15
2.2.2 Bone marrow-derived dendritic cells 15
2.3 *Parapoxvirus ovis* 15
2.4 Reagents 16
2.5 Enzymes 16
2.6 Antibodies 17
2.7 Protein standards 18
2.8 Buffers, media and solutions 18
2.8.1 Cell culture media 19
2.9 Consumables 20
2.10 Devices 21
2.11 Software and databases 21
3. Methods 22
3.1 Cell culture 22

3.1.1 Generation of FLDC ... 23
3.2 Stimulation of FLDC and keratinocytes ... 23
3.2.1 Stimulation of FLDC ... 23
3.2.2 Stimulation of keratinocytes ... 23
3.3 Enzyme-linked immunosorbent assay (ELISA) ... 24
3.4 Flow cytometry ... 25
3.5 Fluorescence microscopy ... 25
3.5.1 Fluorescence staining ... 25
3.5.2 Fluorescence microscopy ... 26
4. Results ... 27
4.1 Stimulation of dendritic cells and keratinocytes ... 27
4.1.1 Comparison of the production of pro-inflammatory cytokines by dendritic cells and keratinocytes ... 27
4.1.2 Comparison of the production of anti-inflammatory cytokines by dendritic cells and keratinocytes ... 29
4.1.3 Effect of PPVO stimulation on the expression of surface markers of FLDC and keratinocytes ... 30
4.2 PPVO-mediated cytotoxic effects on dendritic cells and keratinocytes ... 36
4.3 Detection of PPVO in FLDC and keratinocytes ... 41
5. Discussion ... 44
References ... 48
Danksagung ... 53

List of figures

Figure 1: TNF-α production by FLDC in response to PPVO 27
Figure 2: TNF-α production by keratinocytes in response to PPVO 28
Figure 3: IL-1β production by keratinocytes in response to PPVO 29
Figure 4: IL-10 secretion by FLDC in response to PPVO 29
Figure 5: Gating strategy for the detection of surface markers on cDC 31
Figure 6: Expression of CD86 (A) and MHC-II (B) on FLDC in response to PPVO 32
Figure 7: Gating strategy for the detection of surface markers on keratinocytes 32
Figure 8: Expression of MHC-II on keratinocytes in response to PPVO 33
Figure 9: Expression of MHC-I on keratinocytes in response to PPVO 34
Figure 10: Expression of ICAM-1 on keratinocytes in response to PPVO 35
Figure 11: Expression of PD-L1 on keratinocytes in response to PPVO 36
Figure 12: Gating strategy for the detection of early apoptosis in pDC and cDC 37
Figure 13: Viability of pDC and cDC in response to PPVO 38
Figure 14: Gating strategy for the detection of apoptotic rates in keratinocytes 39
Figure 15: Viability of keratinocytes in response to PPVO 40
Figure 16: Detection of PPVO in FLDC 41
Figure 17: PPVO uptake in keratinocytes 42
Figure 18: Percentage of FLDC (A) and keratinocytes (B) associated with fluorescently labeled PPVO 43

List of tables

Table 1: Antibodies for flow cytometry 17
Table 2: Antibodies for immunofluorescence (IF) 17
Table 3: Capture antibodies for ELISA 17
Table 4: Detection antibodies for ELISA 17
Table 5: Protein standards for ELISA 18
Table 6: Cell culture conditions 22
Table 7: Concentrations of stimuli for the stimulation of FLDC 23
Table 8: Concentrations of stimuli for the stimulation of keratinocytes 24

1. Introduction

1.1 *Parapoxvirus ovis* and the innate immune system

Parapoxvirus ovis (PPVO) is an epitheliotropic virus belonging to the genus *parapoxvirus* within the family of poxviridae. It is a double-stranded DNA virus with a genome size of 140 kb. Unique for PPVO within the group of poxviruses is its high GC content (Wittek *et al.,* 1979). The genome consists of approximately 130 genes most of which are essential for virus replication, packaging and export (Haig, 2006). The PPVO genome also encodes some proteins with strong immunomodulatory properties which have been subject of research for many years. The *F1L* gene is one immunomodulatory factor expressed by PPVO. F1L is a heparin-binding protein and plays a role in virus binding to its host cells thereby initiating the infection cycle (Scagliarini *et al.,* 2004). In the present study F1L was used as target protein for immunofluorescent staining of PPVO within dendritic cells and keratinocytes. Another immunomodulatory protein expressed by PPVO is the vascular endothelial growth factor E (VEGF-E). VEGF-E increases the number of endothelial cells and keratinocytes in the dermis leading to an improvement of epidermal regeneration (Wise *et al.,* 2012).

Two forms of viral particles can be distinguished – the extracellular enveloped virus and the intracellular mature virus. The first step of infection is the attachment to the cell followed by the fusion of the virus membrane with the plasmamembrane of the host cell. Virus uptake by the cell can be realized by various mechanisms, e.g. internalization (Payne and Norrby, 1978) or endocytosis (Vanderplasschen *et al.,* 1998). PPVO, as all poxviruses, replicates in the cytosol of the host cell (Pospischil and Bachmann, 1980), especially in regenerating epidermal keratinocytes (McKeever *et al.,* 1988). For Vaccinia virus (VACV), which is related to PPVO, it is described that the sites of viral transcription and DNA replication, known as viral factories, are enclosed by the membranes of the endoplasmic reticulum (Tolonen *et al.,* 2001). Newly synthesized VACV particles are transported to the outer membrane of the host cell via microtubuli and actin filaments and released via exocytosis (Smith *et al.,* 2002). The exact infection pathway of PPVO is not fully understood but is supposed to be similar to VACV.

Due to its immunostimulatory properties, PPVO can be used as a vaccine vector. For example, the PPVO strain D1701 has been used to express glycoproteins of pseudorabies virus in a non-permissive mouse model. The PPVO vector was shown to express the glycoproteins that stimulated the humoral and cellular immunity in the mouse model. A protective immune response to pseudorabies virus was induced (Fischer *et al.,* 2003).

PPVO can survive in the environment for years which contributes to the high morbidity of orf, the disease caused by PPVO (Haig *et al.*, 1997). Orf (contagious ecthyma, contagious pustular dermatitis, scabby mouth) is a debilitating skin disease most common among ruminants. The disease is characterized by mucosal and skin lesions, pustules and abrasions. Mostly young animals are infected and first infections are most severe, especially around the mouth and nares. Also humans with direct contact to diseased animals can be infected with PPVO. (Haig and Mercer, 1998). In immunocompetent hosts, orf is locally restricted to the epithelium and no systemic spread occurs (Haig, 2006). But in immunosuppressed patients following transplantation or in case of immunodeficiency diseases, atypical and relapsing forms of PPVO infection occur with increasing frequencies (Dal Pozzo *et al.*, 2005).

1.2 Dendritic cells in anti-viral immunity

Dendritic cells (DC) are professional antigen-presenting cells playing an important role in connecting the innate and adaptive immune system. They circulate in the periphery, e.g. in the epidermis, and are the first line of defense against invading pathogens. When they get in contact with pathogens, they phagocytose them and present the processed antigens on their surface. Interaction with pathogens leads to the activation of DC. Activated DC migrate from the periphery to the lymph nodes where they get in contact with naïve T cells. Via MHC and co-stimulatory molecules, DC activate T cells and induce an adaptive immune response (Steinman and Inaba, 1999).

Two subpopulations of DC can be distinguished – plasmacytoid (pDC) and conventional DC (cDC). cDC are characterized by the typical asteroid morphology and fulfill the main functions of DC such as antigen processing and presentation. They are identified by the expression of CD11c, CD11b and the lack of B220. pDC, in contrast to that, are more roundly shaped and are characterized by the expression of CD11c and B220 but lack of CD11b. DC can be generated *in vitro* from bone marrow. In presence of fms-like tyrosine kinase 3-ligand (Flt3L), a mixed population of cDC and pDC is generated (Wick, 2007).

For the successful induction of an immune response, the recognition of pathogen-associated molecular patterns by specific receptors is essential. Different groups of pathogens are recognized by different pattern recognition receptors (PRR). One class of PRR are the toll-like receptors (TLR).

In this study, I focused on the interactions of DC with viruses, especially *Parapoxvirus ovis* (PPVO). pDC recognize PPVO by endosomal TLR9 (manuscript in revision).

An anti-viral mechanism triggered by DC is the release of type I interferons (IFN-α and β). The production of type I interferons prevents viral replication in the host cells and stimulates NK cells, enhances the activation of DC and induces an adaptive immune response (Kawai and Akira, 2006). Both DC subpopulations, cDC and pDC, were shown to produce type I interferons in response to stimulation with inactivated PPVO (iPPVO) (Siegemund *et al.,* 2009). Besides type I interferons, also the type III interferon IFN-λ is released by DC, e.g. in response to Sendai virus and Herpes simplex virus mediating an anti-viral immune response (Ank *et al.,* 2008). DC do not only respond to viral infection with the release of interferons, but also with the production of pro-inflammatory cytokines (e.g. IL-12 family members) (Friebe *et al.,* 2004), that enhance the immune response.

1.3 Keratinocytes as target cells for PPVO infection

Under physiological conditions keratinocytes slowly proliferate in the basal layer of the skin and differentiate in the suprabasal layers. Infection with pathogens or mechanic injury triggers the activation of keratinocytes. Keratinocyte activation is induced and regulated by cytokines and growth factors. IL-1 plays the initial role in this process triggering the proliferation and migration of keratinocytes (Kupper, 1990). The single steps of the activation cycle can be characterized by the expression of certain keratins. Activated keratinocytes express keratin (K) 6, K16 and K17. The activation status of keratinocytes is further characterized by hyperproliferation, migration and changes in the cytoskeleton and the expression of surface molecules. By producing cytokines and chemokines upon infection, they function as non-professional immune cells and are able to alert fibroblasts, endothelial cells, lymphocytes and neighboring keratinocytes (Freedberg *et al.,* 2001).

For the PPVO-related VACV it was found that infected keratinocytes upregulate the secretion of pro-inflammatory cytokines (e.g. IL-6, IL-12p40) (Liu *et al.,* 2005). In a model of keratinocyte raft cultures it was shown that PPVO replicates in epithelial cells. Replication was validated by balloon degeneration and the occurrence of inclusion bodies in the cytoplasm, which is characteristic for PPVO-infected keratinocytes. Six days post-infection, the differentiated epithelium was completely destructed (Dal Pozzo *et al.,* 2005).

In ovine turbinate cells, PPVO was found to be punctually distributed in the cytoplasm (Diel *et al.,* 2011). The PPVO-expressed VEGF-E was observed to induce the re-epithelialization of wounds in a mouse model. Here, the numbers of keratinocytes in the skin increased (Wise *et*

al., 2012). Because the PPVO-induced activation state of murine keratinocytes is largely unknown, this should be investigated during my study and compared to the activation of DC.

1.4 Aim of the study

PPVO as epitheliotropic virus causes orf which is characterized by skin lesions and balloon degeneration of epithelial cells. Previous studies revealed that PPVO activates DC and replicates in epidermal keratinocytes. In my study, the responses of both cell types should be investigated and compared to each other to increase the understanding of PPVO infection in non-permissive hosts. Murine bone marrow-derived dendritic cells as well as murine keratinocytes were analyzed regarding the upregulation of surface markers and the production of cytokines to gain information about their PPVO-induced activation state. The results obtained were different between the two cell types. To explain these differences, the PPVO-mediated cytotoxicity was investigated by annexin-V/7-AAD staining. Additionally, the magnitude of the uptake of PPVO into the cells was analyzed by fluorescence microscopy and compared between DC and keratinocytes.

The analysis of interactions of PPVO with its target cells will help to understand the infection pathway of PPVO. Thus, deeper understanding of PPVO infection could improve therapeutic approaches to reduce the morbidity of orf. In particular, it would be of great importance to prevent lambs and immunocompromised individuals from being infected with PPVO.

Furthermore, a better understanding of interactions of PPVO with non-permissive host cells could increase the usability of PPVO as a vaccine vector.

2. Materials

2.1 Mice

C57BL/6 wild-type mice were kept under specific pathogen-free conditions at the mouse facility of the Max Planck Institute for Evolutionary Anthropology (Leipzig, Germany). Mice were kept according to the guidelines of the Animal Care Usage Committee of the Regierungspräsidium Leipzig, Germany. Female mice at an age of 8-12 weeks were used. Food and water were given *ad libitum*.

2.2 Cells

2.2.1 Murine keratinocytes

Organism:	C57BL/6 mouse
Origin:	epidermis
	adherent

The cells were gained from epithelia of newborn mice, kept in culture and spontaneously immortalized keratinocytes were selected. Keratinocytes were kindly provided by Prof. Dr. T. Magin and prepared by Gabi Baumbach (AG Prof. Magin, University of Leipzig).

2.2.2 Bone marrow-derived dendritic cells

Organism:	C57BL/6 mouse
Origin:	bone-marrow
	non-adherent

Dendritic cells were generated in presence of fms-like tyrosine kinase 3-ligand (Flt3L) and are therefore named Flt3L-derived dendritic cells (FLDC).

2.3 Parapoxvirus ovis

Highly purified PPVO was a kind gift of Prof. Dr. Mathias Büttner (Bayerisches Landesamt für Gesundheit und Lebensmittelsicherheit, Oberschleissheim).

2.4 Reagents

Annexin V Apoptosis Detection Kit APC	ebioscience, Frankfurt/Main, Germany
β-mercaptoethanol	Sigma-Aldrich, Taufkirchen, Germany
collagen I [4.1 mg/mL]	Corning, New York, USA
CpG-ODN 2216	TIB MOLBIOL Syntheselabor GmbH, Berlin, Germany
DMSO	Sigma-Aldrich, Taufkirchen, Germany
FBS	Gibco, Darmstadt, Germany
Fixable Viability Dye eFluor® 780	ebioscience, Frankfurt/Main, Germany
Flt3L	Miltenyi, Bergisch Gladbach, Germany
formaldehyde	Carl Roth GmbH, Karlsruhe, Germany
Hoechst33342 (Molecular probes®)	life Technologies, Carlsbad, USA
L-Glutamin (200 mM)	Sigma-Aldrich, Taufkirchen, Germany
mounting medium Aqua Poly/Mount	Polysciences Inc., Eppelheim, Germany
penicillin/streptomycin	Sigma-Aldrich, Taufkirchen, Germany
sodium pyruvate	Sigma-Aldrich, Taufkirchen, Germany
trypan blue	Sigma-Aldrich, Taufkirchen, Germany

2.5 Enzymes

Trypsin/EDTA	GE Healthcare Europe GmbH, Freiburg, Germany
Streptavidin-coupled horse radish peroxidase	Southern Biotech, Birmingham, USA

2.6 Antibodies

Table 1: Antibodies for flow cytometry

antibody	isotype	labeling	concentration	application	company
anti-ms PD-L1	rat IgG2a	PE	0.2 mg/mL	0.5 µg/1E6 cells	BD Pharmingen, Heidelberg
anti-ms I-A/I-E	rat IgG2b	Alexa 700	0.5 mg/mL	0.25 µg/1E6 cells	BioLegend, Fell
anti-ms H-2D^b	mouse IgG2a	PE	0.2 mg/mL	0.25 µg/1E6 cells	BD Pharmingen, Heidelberg
anti-ms CD86	rat IgG2a	PerCP	0.2 mg/mL	0.25 µg/1E6 cells	BioLegend, Fell
anti-ms CD54	arm. hamster IgG	biotin	0.5 mg/mL	0.25 µg/1E6 cells	BD Pharmingen, Heidelberg
anti-ms CD11b	rat IgG2b	FITC	0.5 mg/mL	0.25 µg/1E6 cells	eBioscience, Frankfurt
anti-ms CD45R	rat IgG2a	eFluor450	0.2 mg/mL	0.5 µg/1E6 cells	eBioscience, Frankfurt

ms: mouse, I-A/I-E: MHC-II, H-2D^b: MHC-I, arm.: Armenian, CD54 = ICAM-1, CD45R = B220, PE: phycoerythrin, Alexa 700 = Alexa Fluor 700, PerCP: peridinin chlorophyll, FITC: fluorescein isothiocyanat.

Table 2: Antibodies for immunofluorescence (IF)

antibody	isotype	labeling	concentration	application	company
anti-PPVO envelope protein F1L	mouse IgG2a	unlabeled	0.2 mg/mL	1:200	Santa Cruz, Heidelberg
anti-ms IgG	donkey IgG	Cy2	0.5 mg/mL	1:1000	dianova, Hamburg

ms: mouse, PPVO: *Parapoxvirus ovis*, Cy2: cyanine

Table 3: Capture antibodies for ELISA

antibody	clone/lot	application	company
anti-ms TNF-α	TN3-19.12	1:250	eBioscience, Frankfurt
anti-ms IFN-α	RMMA-1	1 µg/mL	R&D Systems, Wiesbaden
anti-ms IFN-β	RMMB-1	1 µg/mL	R&D Systems, Wiesbaden
anti-ms IFN-λ	1302378	1 µg/mL	R&D Systems, Wiesbaden
anti-ms IL-12p40	5C3	1:56	Hoffmann La-Roche Ltf., Basel, Switzerland
anti-ms IL-10	E17778-102	1:250	eBioscience, Frankfurt
anti-ms IL-1β	1111047	1 µg/mL	Peprotech, Hamburg
anti-ms IL-6	MP5-20F3	2.5 µg/mL	BD Pharmingen, Heidelberg
anti-ms TSLP	1059552	1:180	R&D Systems, Wiesbaden

ms: mouse

Table 4: Detection antibodies for ELISA

antibody	clone/lot	labeling	application	company
polyclonal rabbit anti-ms IFN-α	-	purified	1:2000	R&D Systems, Wiesbaden
polyclonal rabbit anti-ms IFN-β	-	purified	1:1000	R&D Systems, Wiesbaden
anti-ms IFN-λ	1302378	biotin	1:200	R&D Systems, Wiesbaden
anti-ms IL-12p40	-	biotin	1:800	Hoffmann La-Roche Ltd., Basel, Switzerland
anti-ms IL-10	E17778-102	biotin	1:250	eBioscience, Frankfurt
anti-ms IL-1β	1111047	biotin	0.4 µg/mL	Peprotech, Hamburg
anti-ms IL-6	MP5-20F3	biotin	2.5 µg/mL	BD Pharmingen, Heidelberg
anti-ms TSLP	1059552	biotin	1:180	R&D Systems, Wiesbaden

ms: mouse

2.7 Protein standards

Table 5: Protein standards for ELISA

protein standard	clone/lot	starting concentration	company
recombinant ms IFN-α	-	8000 EU/mL	R&D Systems, Wiesbaden
recombinant ms IFN-β	-	4 ng/mL	R&D Systems, Wiesbaden
recombinant ms IFN-λ	1302378	20 ng/mL	R&D Systems, Wiesbaden
recombinant ms IL-12p40	-	20 ng/mL	Hoffmann La-Roche Ltd., Basel, Switzerland
recombinant ms IL-10	E17778-102	5 ng/mL	eBioscience, Frankfurt
recombinant ms IL-1β	1111047	10 ng/mL	Peprotech, Hamburg
recombinant ms IL-6	MP5-20F3	2.5 µg/mL	BD Pharmingen, Heidelberg
recombinant ms TSLP	1059552	4 ng/mL	R&D Systems, Wiesbaden

ms: mouse

2.8 Buffers, media and solutions

10x PBS	8.0 g NaCl
	0.2 g KCl
	1.83 g Na_2HPO_4
	0.2 g KH_2PO_4
	aqua dest. ad 1 L
	pH = 7.4
Carbonate buffer (ELISA)	17.3 g $NaHCO_3$
	8.6 g Na_2CO_3
	aqua dest. ad 1 L
	pH = 9.5
ELISA blocking buffer	0.1 % gelatin
	0.5 % BSA
	1x PBS ad 1 L
ELISA washing buffer	1x PBS with 0.05 % Tween

Erythrocyte lysis buffer	150 mM NH_4Cl 8 mM $KHCO_3$ 2 mM EDTA (0.5 M) aqua dest. ad 1 L
FACS buffer	3 % FBS 0.1 % NaN_3 (10 %) 1x PBS
IF-permeabilization buffer	1x PBS 1 % FBS 0.2 % Triton-x 100
IF-washing buffer	1x PBS 1 % FBS
Paraformaldehyde	2 % in PBS
Serum diluent (ELISA)	0.1 % gelatin 0.5 % BSA 0.05 % Tween 1x PBS ad 1 L

2.8.1 Cell culture media

RPMI	RPMI 1640 medium (Biochrom) with 10 % FBS 2 mM stable glutamine 1 % P/S

FLDC medium	RPMI supplemented with 10 % FBS 2 mM stable glutamine 1 % P/S 1 mM sodium pyruvate 50 µM β-mercaptoethanol 300 ng/mL Flt3L
Keratinocyte medium	DMEM/Ham's F12 10 % chelex-treated FBS 2 mM Glutamax 100 U/mL sodium-pyruvate 0.5 % P/S 0.18 mM adenine 10 ng/mL EGF 5 µg/mL insulin 0.5 µg/mL hydrocortisone 100 pM choleratoxin

Keratinocyte medium was kindly provided by Prof. T. Magin and prepared by Gabi Baumbach (AG Prof. Magin, University of Leipzig).

2.9 Consumables

cell culture dish 10 cm diameter	Schubert, Leipzig
cell culture flask 25 cm^2, 75 cm^2	VWR, Darmstadt
glass coverslips	VWR, Darmstadt
polylysine-coated glass slides	Carl Roth, Karlsruhe
gloves	Schubert, Leipzig
multi well plates 12-well, 24-well, 96-well	VWR, Darmstadt
parafilm	VWR, Darmstadt
pipet tips	Schubert, Leipzig
pipet tips Rainin	Diagonal, Münster
reaction tubes 1.5 mL, 2.0 mL	Schubert, Leipzig
reaction tubes 15 mL, 50 mL	VWR, Darmstadt

2.10 Devices

Allegra X-22R centrifuge	Beckman-Coulter, Krefeld
Axiovert 25 microscope	Carl Zeiss Microscopy, Jena
Biological Safety Cabinet Class II	NuAire, Plymouth, USA
Centrifuge 5417R	eppendorf, Hamburg
CO_2 incubator 32°C, 37°C	Heraeus Instruments, Hanau
flow cytometer LSRfortessa	BD, Heidelberg
fluorescence microscope OLYMPUS IX-81	Olympus, Hamburg
freezer	Thermo Scientific, Waltham, USA
Hera Safe	Heraeus Instruments, Hanau
Mini centrifuge GMC-060	LMS Group, Tokyo, Japan
mini gyro-rocker SSM3	Stuart Equipment, Staffordshire, UK
pipets	eppendorf, Hamburg
Pipetus®	VWR GmbH, Darmstadt
precision microplate reader	Molecular Devices, Biberach
Rainin pipets	Mettler Toledo GmbH, Gießen
scale PM4000	Mettler Toledo GmbH, Gießen
thermomixer 5436	eppendorf, Hamburg
Vortex Genie 2	Scientific Industries, New York, USA
Wellwash AC	Thermo Labsystems, Milford, USA
Zeiss LSM 780 confocal microscope	Carl Zeiss Microscopy, Jena

2.11 Software and databases

Adobe Reader XI	Adobe Systems, San Jose, USA
AnalySIS^{D}	Olympus, Hamburg
Citavi 4.3.0.15	Swiss Academic, Wädenswil, Schweiz
GraphPad Prism v5.01	GraphPad Software, La Jolla, USA
Microsoft Office® Professional Plus 2010	Microsoft, Redmond, USA
SoftMax Pro v5.0	Molecular Devices, Sunnyvale, USA
Zen Software 2010	Carl Zeiss Microscopy, Jena

3. Methods

3.1 Cell culture

All cells were cultivated in cell-specific culture media indicated in Table 6.

Keratinocytes were grown on cell culture plastic dishes with 10 cm diameter in a humidified atmosphere at 32°C and 5 % CO_2. Dishes were pre-coated with collagen I-solution (0.5 mL stock solution [4.1 mg/mL] diluted in 42.7 mL 0.2 N acetic acid) for 30 min at 37°C and washed twice with PBS before cell suspension was added. For passaging, the medium was aspired, the cells were washed with PBS and incubated with trypsin/EDTA for 15 min at 37°C to detach the cells. Keratinocytes were split 1:2 every 3 to 4 days.

FLDC were generated from bone marrow of female C57BL/6 mice (see chapter 3.1.1 Generation of FLDC) and grown in FLDC medium at 37°C in a humidified atmosphere with 5 % CO_2.

For passaging and seeding, all cells were detached by resuspending in medium and transferred to a 15 mL tube. An aliquot of the cell suspension was supplemented with trypan blue and the cell number was determined with a Neubauer chamber. All squares were counted and the cell number per mL was calculated.

Table 6: Cell culture conditions

cells	medium	supplements	conditions
FLDC	RPMI medium	10 % FBS 2 mM stable glutamine 1 % P/S 1 mM Na-pyruvate 50 µM β-mercaptoethanol 300 ng/mL Flt3L	37°C 5 % CO_2
keratinocytes	DMEM/Ham's F12	10 % chelex-treated FBS 2 mM Glutamax 100 U/mL Na-pyruvate 0.5 % P/S 0.18 mM adenine 10 ng/mL EGF 5 µg/mL insulin 0.5 µg/mL hydrocortisone 100 pM choleratoxin	32°C 5 % CO_2

FBS: foetal bovine serum, P/S: penicillin/streptomycin, FLDC: Flt3L-derived dendritic cells, Na-pyruvate: sodium pyruvate, Flt3L: Fms-related tyrosine kinase 3-ligand, EGF: epidermal growth factor.

3.1.1 Generation of FLDC

C57BL/6 mice were dissected and bone marrow was washed out of the thigh bones with FACS buffer and collected in 50 mL tubes. The tubes were centrifuged for 8 min at 300 g and the supernatants were discarded. Erythrocyte lysis buffer was added to the suspension and incubated for 45 s. The reaction was stopped with PBS and the suspension was centrifuged again (8 min, 300 g). The supernatant was discarded and the pellet was taken up in RPMI medium. The cell number was determined using a Neubauer chamber. For generating a mixture of plasmacytoid DC (pDC) and conventional DC (cDC), 1.7×10^6 cells per mL were seeded in cell culture flasks with FLDC medium and cultivated at 37°C and 5 % CO_2. After 8 days of incubation, the cells were counted again and seeded into well plates for stimulation.

3.2 Stimulation of FLDC and keratinocytes

3.2.1 Stimulation of FLDC

5×10^5 FLDC per well were seeded in 24-well plates in a total volume of 500 µl. Stimuli (Table 7) were added directly to the medium and the stimulated cells were incubated for 24 hours. Cell suspensions were collected and centrifuged for 5 min at 400 g. The supernatants were collected and stored at -20°C until cytokine analysis by ELISA was done (see chapter 3.3 Enzyme-linked immunosorbent assay (ELISA)). The cells were washed and prepared for immuno-fluorescence (see chapter 3.5.1 Fluorescence staining) or flow cytometry (see chapter 3.4 Flow cytometry).

Table 7: Concentrations of stimuli for the stimulation of FLDC

stimulus	stock concentration	final concentration
CpG-ODN 2216	100 µM	1 µM
iPPVO wt strain D1701	1×10^9 particles per mL	MOI 10 (10 particles per cell)
vPPVO wt strain D1701	1×10^9 particles per mL	MOI 10 (10 particles per cell)

CpG-ODN 2216: CpG-olidodesoxynucleotide, iPPVO: inactivated *Parapoxvirus ovis*, vPPVO: replication-competent ("viable") *Parapoxvirus ovis*, MOI: multiplicity of infection.

3.2.2 Stimulation of keratinocytes

For stimulation, 1.5×10^5 keratinocytes per well in a volume of 1.2 mL were seeded into wells of a 24-well plate. Plates were stored at 32°C until the cells became adherent (2-3 days).

Stimuli were added in a volume of 400 µl. Keratinocytes were infected with replication-competent ("viable") PPVO. As positive control they were stimulated with IFN-γ or a combination of IL-17A/TNF-α. For concentrations see Table 8. As negative control, cells were left unstimulated (medium).

Table 8: Concentrations of stimuli for the stimulation of keratinocytes

stimulus	stock concentration	final concentration
IFN-γ	2 mg/mL	20 ng/mL
IL-17A	25 µg/mL	40 ng/mL
TNF-α	10 µg/mL	20 ng/mL
PPVO	1×10^9 particles per mL	MOI 10 (10 particles per cell)
		MOI 1 (1 particle per cell)

IFN-γ: interferon γ, IL-17A: interleukin 17A, TNF-α: tumor necrosis factor α, PPVO: *Parapoxvirus ovis*, MOI: multiplicity of infection.

3.3 Enzyme-linked immunosorbent assay (ELISA)

Sandwich ELISA was applied for the quantification of cytokines. 96-well plates were coated with 50 µl of specific capture antibodies. Capture antibodies were diluted in PBS (IL-1β) or carbonate buffer (other cytokines) and incubated overnight at 4°C. All other antibodies as well as the protein standards were diluted in serum diluent. All washing steps were carried out with washing buffer. The plates were washed once and then blocked with 250 µl blocking buffer for 2 hours at room temperature. Plates were washed again and the cytokine standard curve and the supernatants were added to the plates and incubated for 2 hours (except IFN-α which was incubated 4 hours). Plates were washed three times and the detection antibody (biotinylated, except for IFN-α and β) was added. After 2 hours of incubation, the plates were washed four times and then incubated with horse radish peroxidase-coupled streptavidin or secondary antibody (for IFN-α and β) for 60 min. Plates were washed five times and 100 µl TMB were added as substrate for the enzymatic reaction. ELISA plates were measured at 650-450 nm until the extinction was 1.5-2. Then, the reaction was stopped with 100 µl H_3PO_4 and the yellow extinction was measured at 450-650 nm. Extinctions were measured with a precision microplate reader (Molecular Devices, Sunnyvale, US) and analyzed with SoftMax Pro v5.0 and GraphPad Prism v5.01.

3.4 Flow cytometry

Keratinocytes: 24 or 72 hours post-infection, the cell culture supernatants were collected for ELISA and the cells were washed with PBS and detached with trypsin/EDTA. The reaction was stopped with FBS and cell suspensions were transferred to 1.5 mL tubes.

FLDC: 24 hours post-infection, cell suspensions were collected and centrifuged 5 min at 400 g. The supernatants were stored at -20°C until analysis by ELISA was done.

All cells were washed twice with PBS. To exclude dead cells from the subsequent analysis, the pellets were resuspended in LD dye (diluted 1:1000 in PBS). Following 20 min of incubation, cells were washed twice with FACS buffer. Pellets were resuspended in antibody mastermixes (Table 1) – one duplicate for the stained sample and one duplicate for the isotype control – and incubated for 30 min in the dark. Cells were washed twice with FACS buffer and incubated with the secondary antibody (streptavidin-FITC) for 30 min in the dark. Cells were washed with FACS buffer and the pellets were resuspended in annexin-V binding buffer. 15 min prior to flow cytometric analysis, 5 µl per well annexin-V (APC-labeled) were added to detect early apoptotic cells.

3.5 Fluorescence microscopy

3.5.1 Fluorescence staining

Keratinocytes: Keratinocytes were grown on collagen I-coated glass coverslips and infected with PPVO or left untreated (medium). 24 or 72 hours post-infection, the supernatants were collected and cells were washed with PBS.

FLDC: FLDC were resuspended in medium, transferred to 1.5 mL tubes and centrifuged for 5 min at 400 g. The supernatants were collected, pellets were resuspended in ice-cold PBS and transferred to poly-L-lysine-coated glass slides. Cell adherence was induced by 15 min incubation at 37°C and followed by washing with PBS.

Fixation was done with 2 % paraformaldehyde for 20 min at 4°C and then washed with PBS. To permeabilize the cells, they were incubated with IF-permeabilization buffer for 5 min on ice followed by washing (3x 10 min) with PBS with 1 % FBS. Cells were incubated with the primary mouse anti-PPVO (anti-PPVO envelope protein F1L) antibody for 60 min. Following another three washing steps (3x 10 min), staining was done with the secondary Cy2-labeled donkey anti-mouse IgG antibody which was incubated for 60 min and followed by incubation with Hoechst33342 for 5 min. The cells were extensively washed with PBS (4x 10 min) and

once with aqua dest. and mounted on glass slides. Samples were stored at 4°C until analysis was done.

3.5.2 Fluorescence microscopy

Stained samples were analyzed with a confocal microscope (LSM 780, Carl Zeiss) with 40x/1.3 or 63x/1.3 oil immersion objectives. Analysis of images was done with Zen Software 2010 (Carl Zeiss). Same settings were used for all samples of each cell type.
Additionally, photographs were taken with a fluorescence microscope (OLYMPUS IX-81) with a 20x/1.0 objective. For quantification, the number of PPVO-stained cells of 5 photographs per sample was determined and divided by the total cell number on each picture.

4. Results

4.1 Stimulation of dendritic cells and keratinocytes

4.1.1 Comparison of the production of pro-inflammatory cytokines by dendritic cells and keratinocytes

Dendritic cells (DC) are among the first sentinels against invading pathogens. As antigen-presenting cells they act as mediators between the innate and adaptive immune system. Thus, it is important to study their response to PPVO. To investigate the activation of these cells by replication-competent PPVO, DC were generated from bone marrow of C57BL/6 mice. In presence of Flt3L, a mixed population of conventional and plasmacytoid dendritic cells is generated (FLDC). FLDC were incubated with 10 virus particles per cell (= multiplicity of infection (MOI) 10), 1 µM CpG-ODN as positive control or left untreated in medium as negative control. 24 hours post-stimulation, the supernatants were collected and analyzed by sandwich ELISA. Figure 1 shows that stimulation with PPVO induced FLDC to produce low levels of TNF-α. Stimulation with the control stimulus CpG-ODN triggered strong TNF-α production, demonstrating the ability of cDC to produce strong cytokine responses.

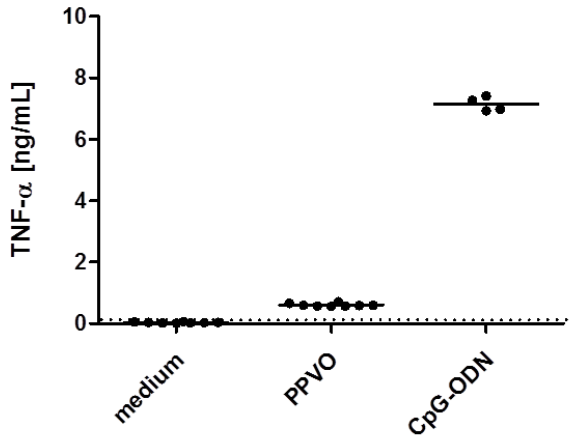

Figure 1: TNF-α production by FLDC in response to PPVO
Cells were infected with MOI 10 and incubated for 24 hours. Concentration of TNF-α was measured with sandwich ELISA. PPVO: replication-competent PPVO (MOI 10), CpG-ODN: positive control, medium: negative control. Dotted line indicates detection limit. One representative of two independent experiments is shown.

To compare the activation of FLDC, which act as first line of defense against invading organisms, to the activation of keratinocytes, which are the cells at the site of PPVO infection, murine keratinocytes were infected with 10 or 1 virus particles per cell (MOI 10 or 1) or stimulated with 20 ng/mL IFN-γ as positive control. 24 or 72 hours post-infection, the cell culture supernatants were collected and analyzed by sandwich ELISA. Murine keratinocytes

constitutively produced low amounts of TNF-α (Figure 2). In response to PPVO infection or cytokine stimulation, no additional TNF-α production was induced. Also, longer incubation times had no effect on the TNF-α secretion by keratinocytes. Compared to FLDC (Figure 1), the secreted cytokine amounts were much lower. Thus, whereas keratinocytes constitutively secrete TNF-α, DC are more potent TNF-α producers in response to PPVO than keratinocytes.

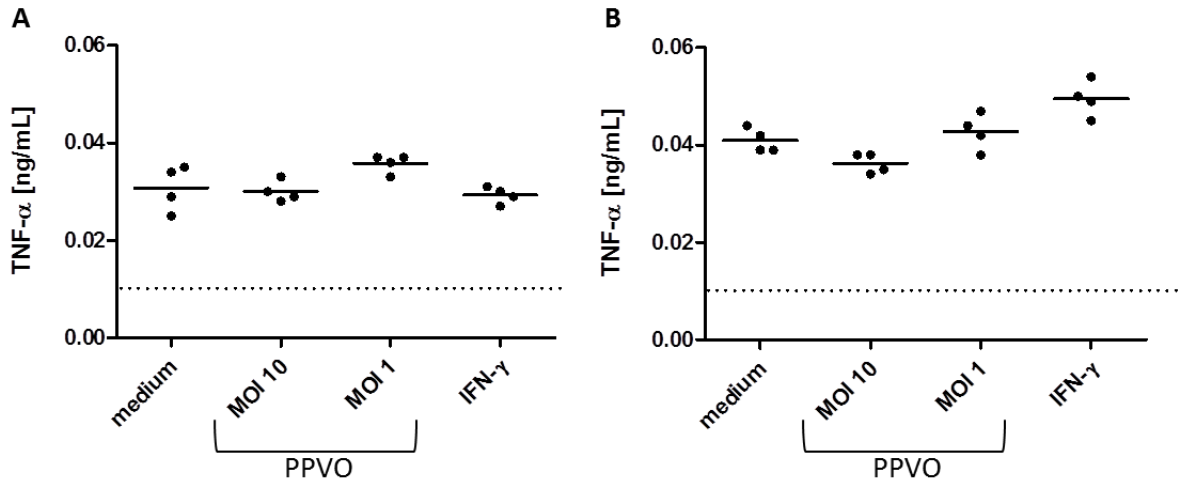

Figure 2: TNF-α production by keratinocytes in response to PPVO
Cells were infected with MOI 10 or 1 and incubated for 24 hours (A) or 72 hours (B). The supernatants were collected and the concentration of TNF-α was measured with sandwich ELISA. PPVO: replication-competent PPVO, MOI: multiplicity of infection, medium: negative control. Dotted line indicates detection limit. One representative of three independent experiments is shown.

IL-1β was analyzed as another pro-inflammatory cytokine being essential for the activation of keratinocytes (Freedberg *et al.*, 2001). Indeed, keratinocytes produced low levels of IL-1β in response to infection with PPVO (MOI 10) after 72 hours (Figure 3b). 24 hours post-infection IL-1β levels were mostly below detection (Figure 3a). FLDC did not produce any IL-1β (data not shown). Thus, PPVO induces TNF-α production in DC but not in keratinocytes, and IL-1β in keratinocytes, but not in DC. These data demonstrate that DC and keratinocytes react differently upon PPVO encounter.

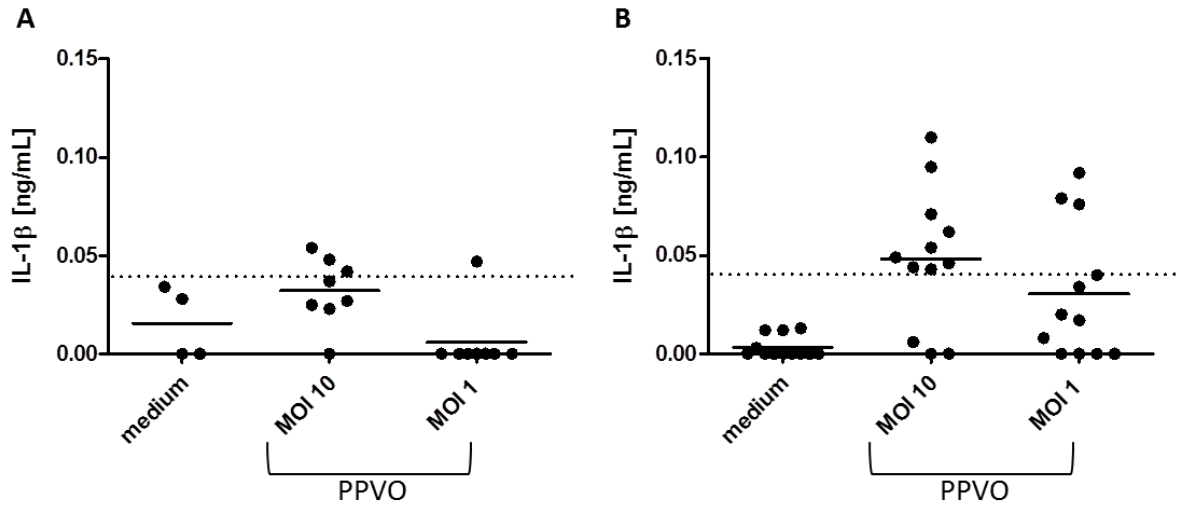

Figure 3: IL-1β production by keratinocytes in response to PPVO
Cells were infected with MOI 10 or 1 and incubated for 24 hours (A) or 72 hours (B). The supernatants were collected and the concentration of IL-1β was measured with sandwich ELISA. PPVO: replication-competent PPVO, MOI: multiplicity of infection, medium: negative control. Dotted line indicates detection limit. One representative of three independent experiments is shown.

4.1.2 Comparison of the production of anti-inflammatory cytokines by dendritic cells and keratinocytes

In the previous chapter, the production of the pro-inflammatory cytokines TNF-α and IL-1β was investigated. Keratinocytes produce IL-10 in response to infection with Herpes simplex virus which has a regulatory effect on immune responses (Halliday *et al.*, 1997). Therefore, IL-10 as representative anti-inflammatory cytokine was analyzed. CpG-ODN-stimulated FLDC produced IL-10. But, infection with PPVO did not induce detectable IL-10 production in FLDC (Figure 4).

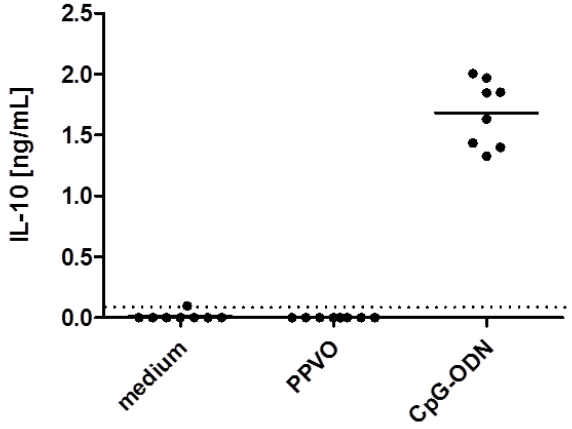

Figure 4: IL-10 secretion by FLDC in response to PPVO
Cells were infected with MOI 10 and incubated for 24 hours. The supernatants were collected and the concentration of IL-10 was measured with sandwich ELISA. PPVO: replication-competent PPVO (MOI 10), CpG-ODN: positive control, medium: negative control. Dotted line indicates detection limit. One representative of two independent experiments is shown.

Keratinocytes did not produce measurable levels of IL-10 either (data not shown). Taken together, these data indicate that PPVO does not induce IL-10 in DC or keratinocytes.

4.1.3 Effect of PPVO stimulation on the expression of surface markers of FLDC and keratinocytes

In addition to the analysis of cytokine secretion by FLDC and keratinocytes, the effect of PPVO stimulation on the expression of surface markers in both cell types was investigated. Cells were stimulated with PPVO and positive control stimuli or left in medium as negative control. After incubation (24 or 72 hours), the cells were stained with fluorescently labeled antibodies and analyzed by flow cytometry. The analysis was focused on viable cells. Figure 5 shows the gating strategy for the analysis of surface markers on FLDC. In the first step cell debris was excluded, followed by the exclusion of doublets by gating FSC-A against FSC-W and SSC-A against SSC-W. The remaining single cells were gated for annexin-V^- and LD dye^- events representing living cells (Figure 5 D). DC were identified by the expression of CD11c. The $CD11c^+$ gate was set according to the respective isotype (Figure 5 E) to avoid unspecific, false-positive signals. The DC subpopulation was further subdivided into $CD11b^+$ $B220^-$ cDC and $CD11b^{low}$ $B220^+$ pDC. The majority of emerging DC belongs to the cDC subpopulation. Here, only 2-3 % of living cells were pDC. Therefore, only cDC were analyzed concerning the expression of surface molecules. For DC, two markers were studied – the antigen-presenting MHC-II and the co-stimulatory molecule CD86. Both positive gates were set according to the isotypes (Figure 5 G and H).

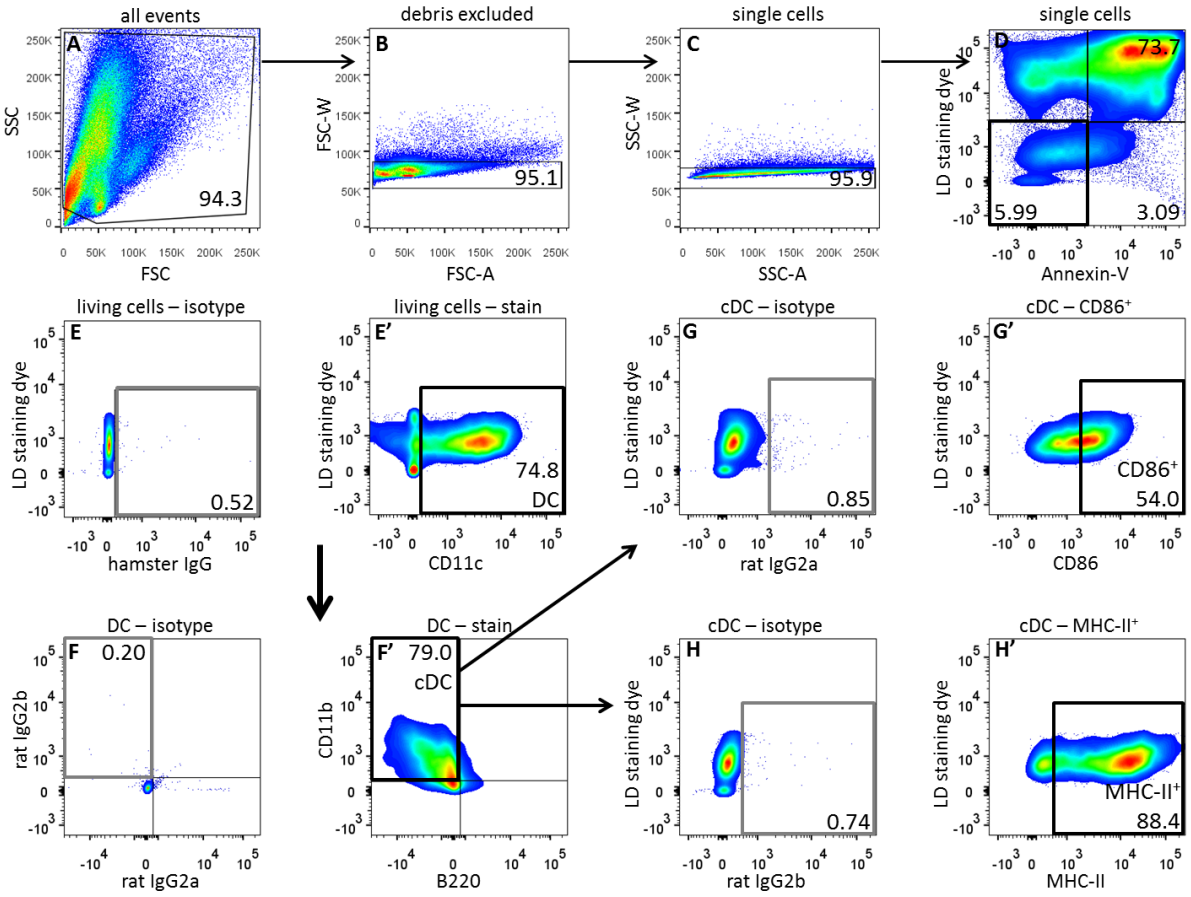

Figure 5: Gating strategy for the detection of surface markers on cDC
A: exclusion of cell debris, **B:** gating FSC-A against FSC-W to exclude doublets, **C:** gating SSC-A against SSC-W to exclude doublets, **D:** gating for annexin-V$^-$ and LD dye$^-$ events representing living cells, **E/E':** gating for CD11c$^+$ cells representing DC, gate is set according to the isotype (E), **F/F':** gating for CD11b$^+$ events representing cDC and B220$^+$ events representing pDC, gates are set according to the isotypes (F), **G/G':** gating for CD86$^+$ cells representing activated cDC, gate is set according to the isotype (G), **H':** gating for MHC-II$^+$ cells representing activated cDC, gate is set according to the isotype (H). CpG-ODN-stimulated cells are shown as example.

Unstimulated cells expressed low levels of CD86. In response to stimulation with PPVO and CpG-ODN, the expression of CD86 strongly increased. In contrast to CpG-ODN stimulation, PPVO did not induce CD86 upregulation on all cells (Figure 6 A).

Mature cDC expressed high levels of MHC-II constitutively (Figure 6 B). In response to both CpG-ODN and PPVO, the expression of this activation marker was profoundly upregulated (Figure 6 B). These data demonstrate that cDC get activated by PPVO.

Keratinocytes reacted differently than FLDC in response to PPVO infection concerning cytokine secretion. Therefore, I was further interested in possible differences in the expression of surface markers between DC and keratinocytes.

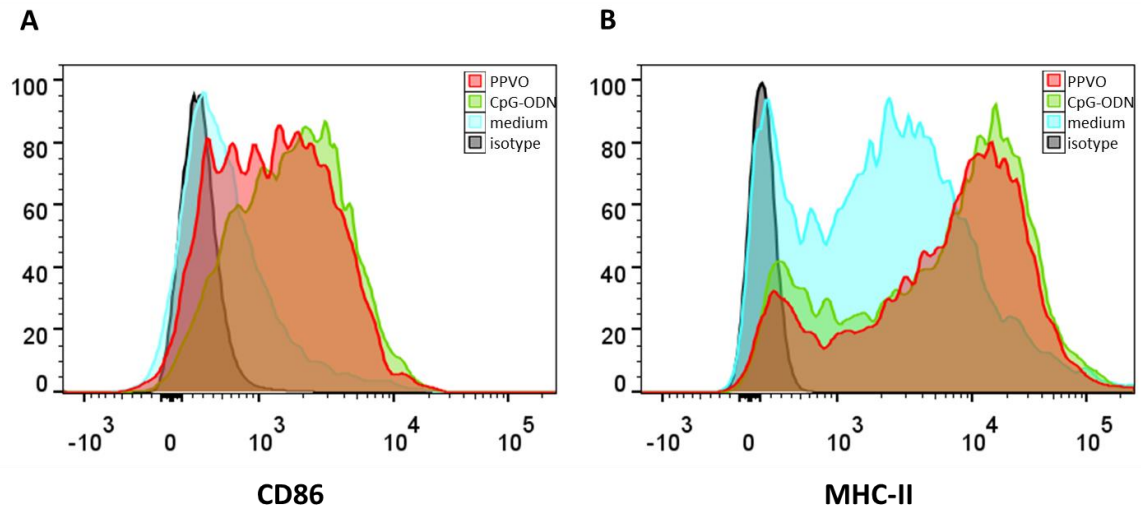

Figure 6: Expression of CD86 (A) and MHC-II (B) on FLDC in response to PPVO
FLDC were infected with PPVO at MOI 10 (red), stimulated with CpG-ODN (green) or left untreated (medium, blue) for 24 hours. Cells were gated as shown in Figure 5 and analyzed for the expression of CD86 (**A**) and MHC-II (**B**) by flow cytometry. The isotype controls are shown in grey. One representative of two independent experiments is shown.

For keratinocytes the same gating strategy was applied as for FLDC (Figure 7). Cell debris and doublets were excluded and by gating for annexin-V$^-$ and LD dye$^-$ events, only living cells were analyzed. These cells were analyzed for the expression of MHC-II, MHC-I, PD-L1 (CD274) and ICAM-1 (CD54). The gates for positive cells were set according to the appropriate isotype controls (Figure 7 E).

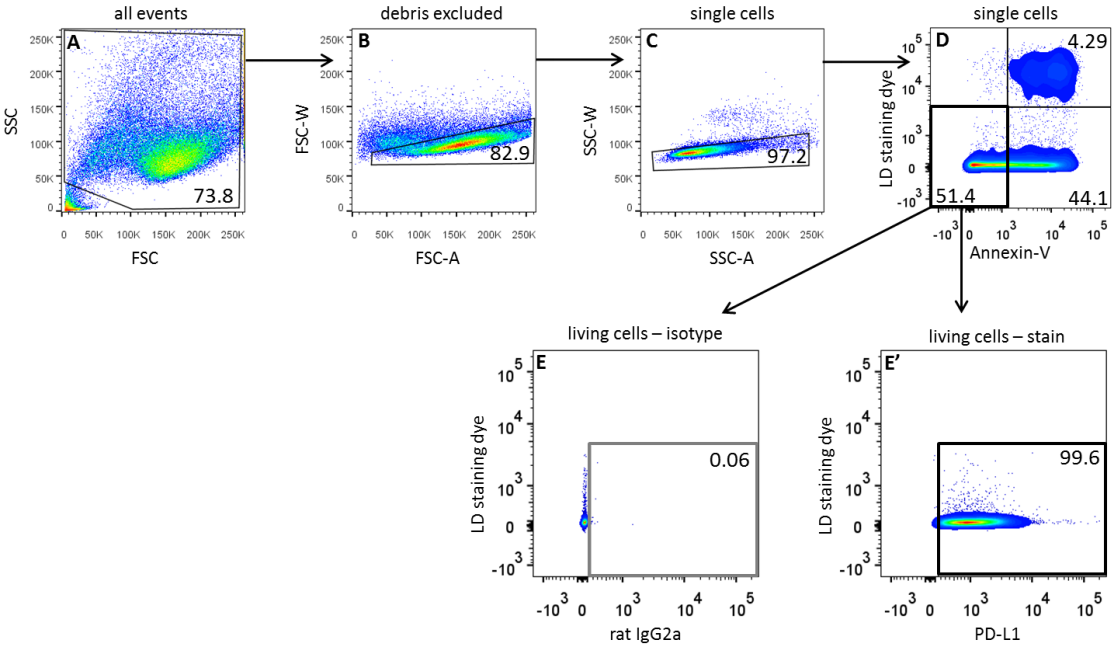

Figure 7: Gating strategy for the detection of surface markers on keratinocytes
A: cell debris was excluded, **B:** gating FSC-A against FSC-W to exclude doublets, **C:** gating SSC-A against SSC-W to exclude doublets, **D:** gating for annexin-V$^-$ and LD dye$^-$ events representing living cells, **E:** gating for positive cells, gate is set according to the isotype control, **E':** positive cells (same gate for isotype control and sample). IFN-γ-stimulated cells expressing PD-L1 are shown as example.

In cDC, the expression of MHC-II is increased upon stimulation with PPVO (Figure 6 B). Keratinocytes are proposed to upregulate MHC molecules in response to inflammatory stimuli and to have the ability to activate T cells (Fan *et al.*, 2003). To investigate that and to compare it to FLDC, MHC-II expression was analyzed on keratinocytes as well. In contrast to FLDC, keratinocytes did not upregulate the expression of MHC-II in response to PPVO infection or stimulation with IFN-γ.

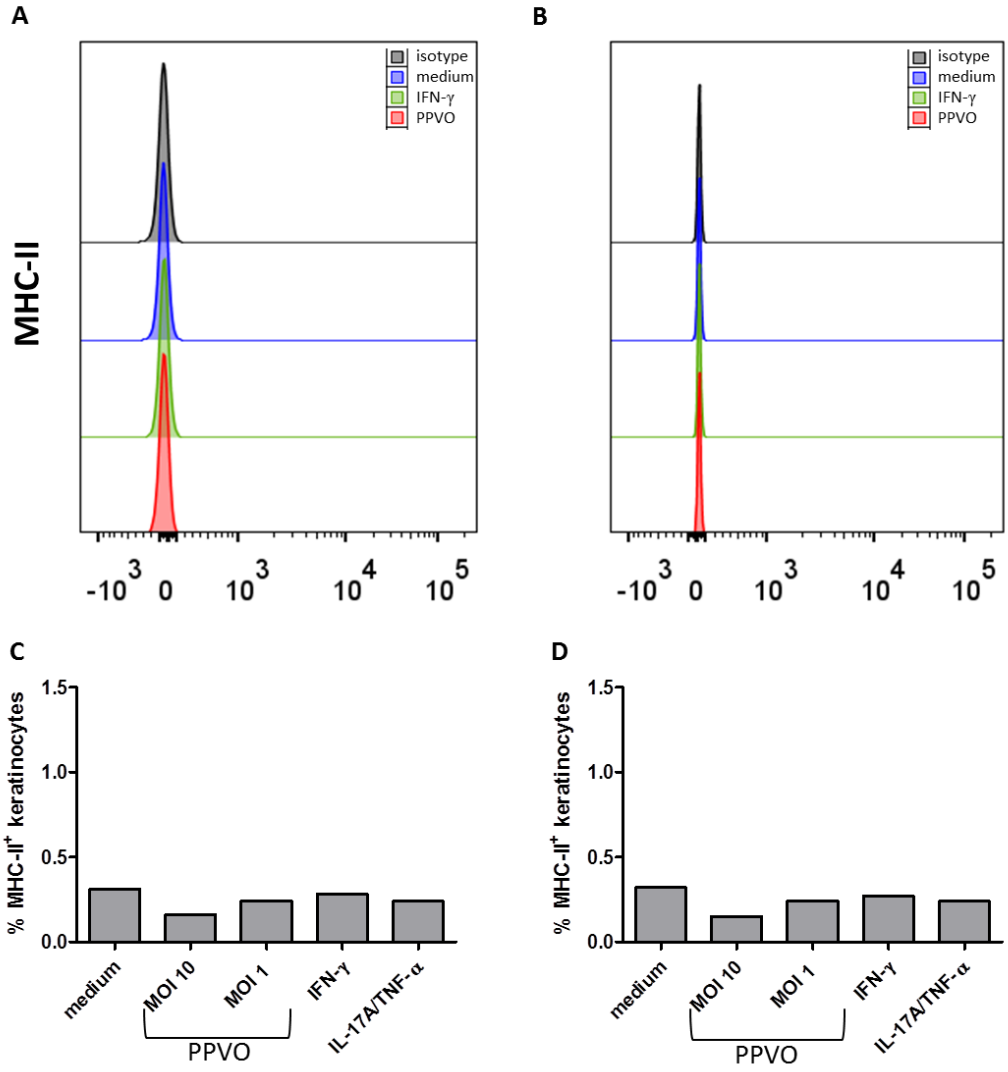

Figure 8: Expression of MHC-II on keratinocytes in response to PPVO
Keratinocytes were infected with PPVO at MOI 10 (**A** and **B** red) or 1, stimulated with IFN-γ (green) or IL-17A/TNF-α or left untreated (medium, blue) and analyzed by flow cytometry for MHC-II expression 24 (**A/C**) or 72 hours (**B/D**) post-infection. Surface expression of MHC-II 24 (**A**) or 72 hours (**B**) post-infection. Percentage of MHC-II-expressing keratinocytes after 24 hours (**C**) and 72 hours (**D**). Stimulation with IL-17A/TNF-α did not induce MHC-II expression. To obtain a sufficient number of flow cytometry events, unique samples had to be analyzed (precluding statistical analysis). One representative of two independent experiments is shown.

Also, the expression of MHC-I on keratinocytes was determined. Figure 9 reveals that keratinocytes expressed low levels MHC-I upon IFN-γ stimulation after 72 hours, but not in response to PPVO.

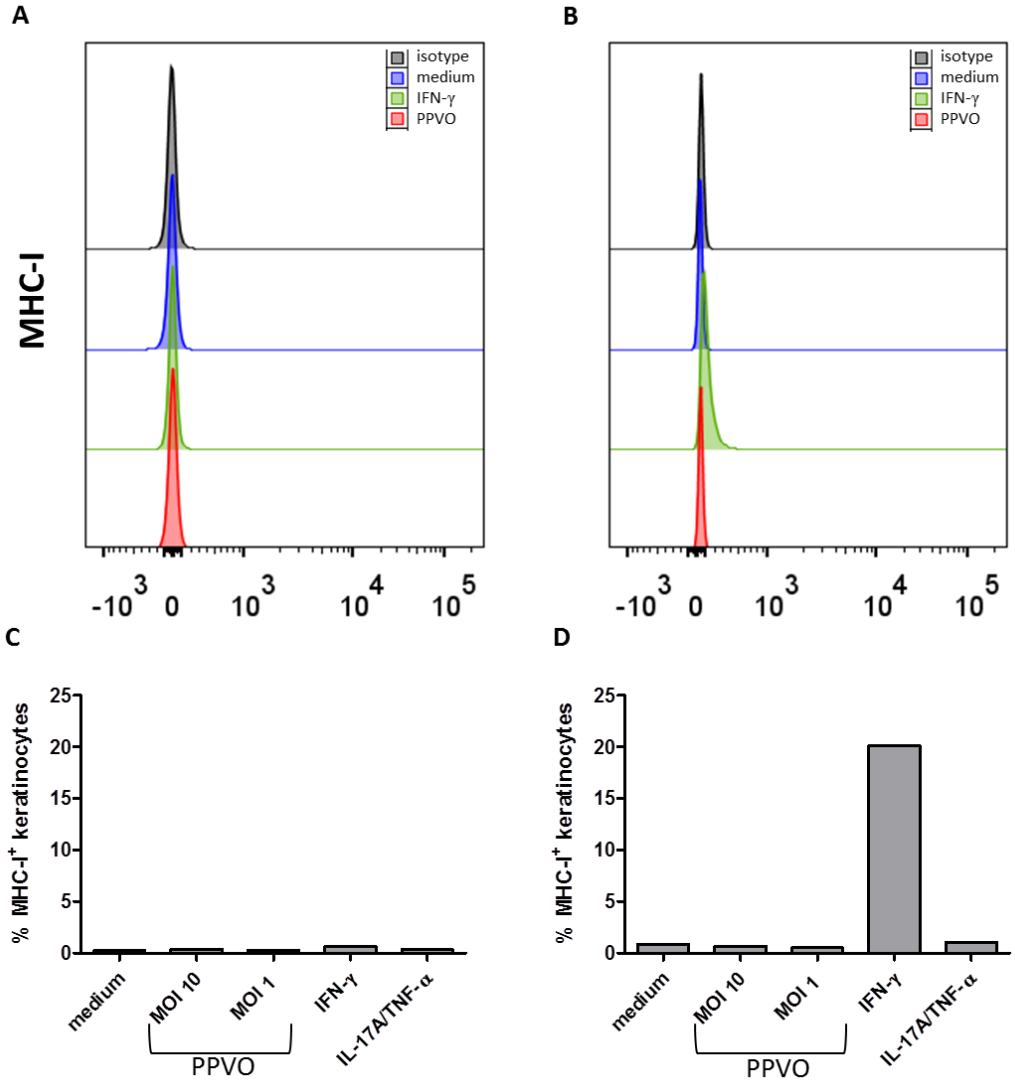

Figure 9: Expression of MHC-I on keratinocytes in response to PPVO
Keratinocytes were infected with PPVO at MOI 10 (**A** and **B** red) or 1, stimulated with IFN-γ (green) or IL-17A/TNF-α or left untreated (medium, blue) and analyzed by flow cytometry for MHC-I expression 24 (**A/C**) or 72 hours (**B/D**) post-infection. Surface expression of MHC-I 24 hours (**A**) or 72 hours (**B**) post-infection. Percentage of MHC-I-expressing keratinocytes after 24 (**C**) and 72 hours (**D**). Stimulation with IL-17A/TNF-α did not induce MHC-I expression. To obtain a sufficient number of flow cytometry events, unique samples had to be analyzed (precluding statistical analysis). One representative of two independent experiments is shown.

ICAM-1 is an activation marker playing a role in interactions between keratinocytes and lymphocytes and is expressed in many skin diseases (Matsunaga *et al.*, 1996). PPVO causes the skin disease orf. Therefore, I was interested in the expression of ICAM-1 by keratinocytes in response to PPVO infection. PPVO infection had no effect on ICAM-1 expression (Figure 10). Stimulation with a combination of IL-17A and TNF-α led to a transient increase in

ICAM-1 expression after 24 hours (Figure 10 A and C) that declined a little bit after 72 hours (Figure 10 B and D). These data indicate that keratinocytes can be activated by cytokine stimulation (IL-17A/TNF-α), but PPVO does not induce elevated ICAM-1 expression on keratinocytes.

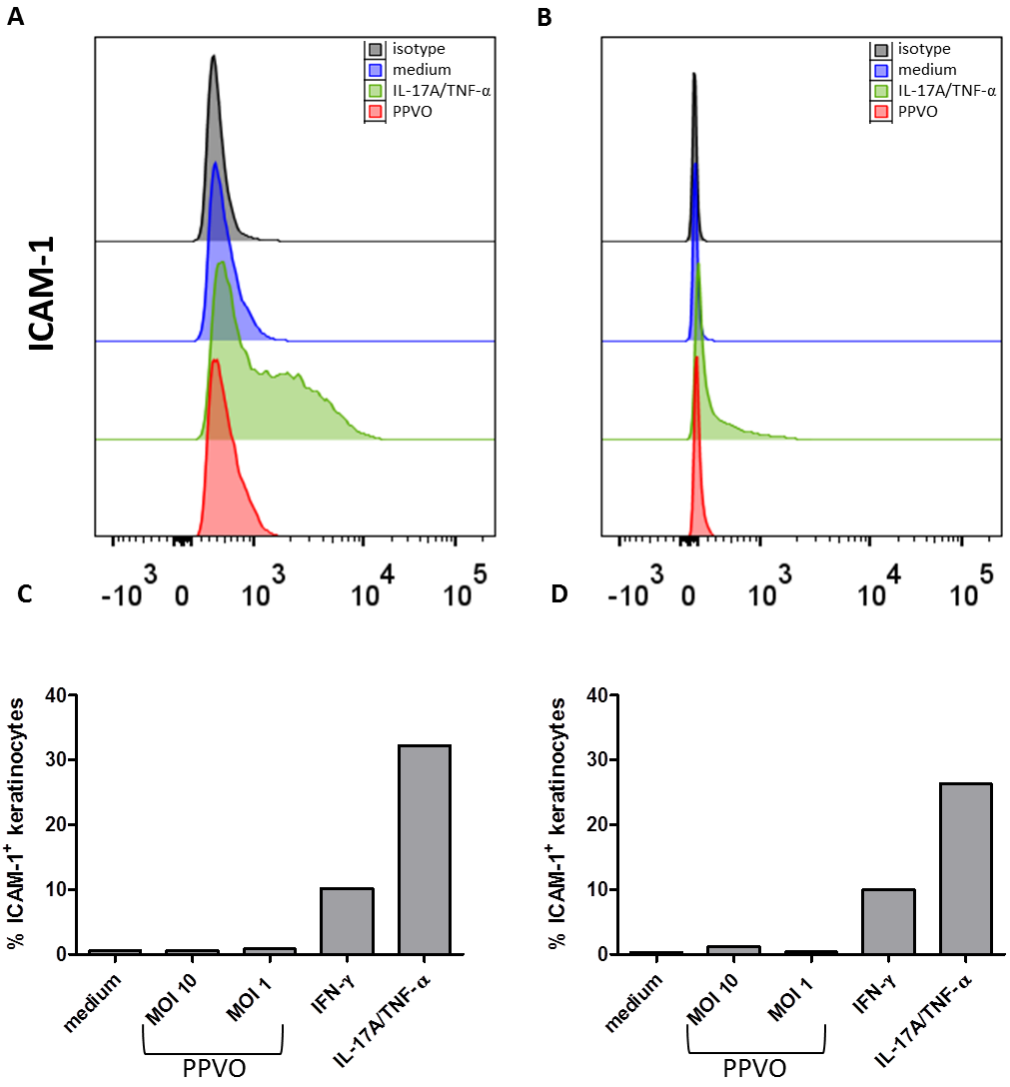

Figure 10: Expression of ICAM-1 on keratinocytes in response to PPVO
Keratinocytes were infected with PPVO at MOI 10 (**A** and **B** red) or 1, stimulated with IFN-γ or IL-17A/TNF-α (green) or left untreated (medium, blue) and analyzed by flow cytometry for ICAM-1 expression 24 (**A/C**) or 72 hours (**B/D**) post-infection. Surface expression of ICAM-1 24 (**A**) or 72 hours (**B**) post-infection. Percentage of ICAM-1-expressing keratinocytes after 24 hours (**C**) and 72 hours (**D**). Stimulation with IFN-γ did not induce ICAM-1 expression. To obtain a sufficient number of flow cytometry events, unique samples had to be analyzed (precluding statistical analysis). One representative of two independent experiments is shown.

It was shown that stimulation with IFN-γ as well as chronic inflammation upregulates the expression of the co-inhibitory molecule PD-L1 on keratinocytes (Peña-Cruz *et al.*, 2010). Therefore, I examined the effects of PPVO infection on the expression of PD-L1 (Figure 11). Unstimulated keratinocytes expressed low levels of PD-L1. Infection with PPVO had no

effect on the expression of PD-L1 on keratinocytes. As expected, stimulation with IFN-γ increased PD-L1 expression (Figure 11). Taken together, the analysis of activation markers suggests that PPVO has no effect on the activation status of keratinocytes.

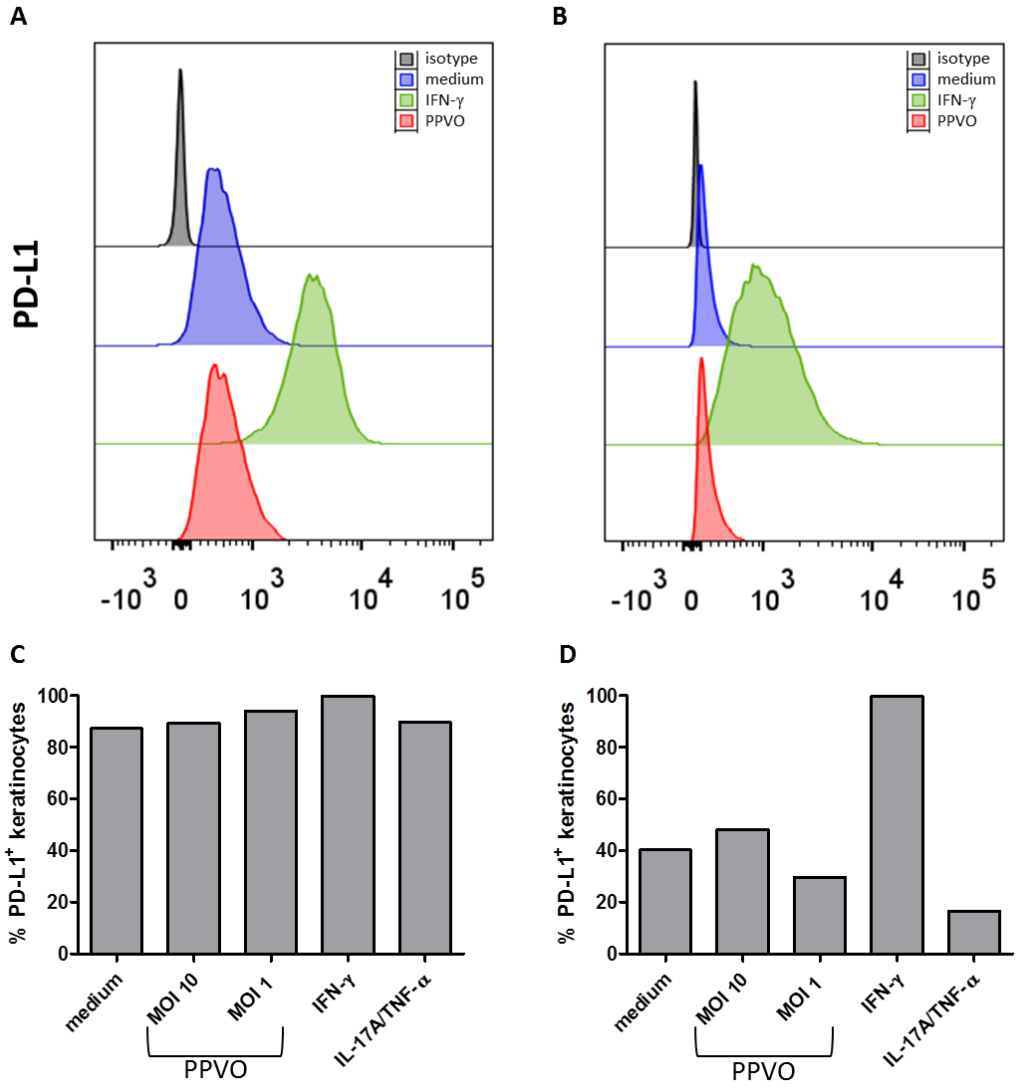

Figure 11: Expression of PD-L1 on keratinocytes in response to PPVO
Keratinocytes were infected with PPVO at MOI 10 (**A** and **B** red) or 1, stimulated with IFN-γ (green) or IL-17A/TNF-α or left untreated (medium, blue) and analyzed by flow cytometry for PD-L1 expression 24 (**A/C**) or 72 hours (**B/D**) post-infection. Surface expression of PD-L1 24 hours (**A**) or 72 hours (**B**) post-infection. Percentage of PD-L1-expressing keratinocytes after 24 (**C**) and 72 hours (**D**). Stimulation with IL-17A/TNF-α did not induce PD-L1 expression. To obtain a sufficient number of flow cytometry events, unique samples had to be analyzed (precluding statistical analysis). One representative of two independent experiments is shown.

4.2 PPVO-mediated cytotoxic effects on dendritic cells and keratinocytes

The analysis of cytokine secretion and surface marker expression revealed fundamental differences between FLDC and keratinocytes. Therefore, I was interested in approaches to explain these differences. Differences in the viability of both cell types following infection

with PPVO could be one explanation. Stimulated FLDC and keratinocytes were stained with annexin-V and Fixable Viability Dye eFluor® 780 (LD dye), to gain insight into differences between FLDC and keratinocytes concerning cell death and apoptosis in response to PPVO. Tests confirmed that the analysis with LD dye provided comparable results to the traditionally known annexin-V/7-aminoactinomycin (7-AAD) staining protocol. However, in contrast to 7-AAD, LD dye does not leave stain traces in the flow cytometer and was therefore chosen for further analysis. The gating strategy for the analysis of the viability of FLDC is depicted in Figure 12. Following cell debris and doublet exclusion, DC were identified with the help of CD11c expression. By gating CD11b against B220, the DC population was further subdivided into cDC and pDC. cDC and pDC were analyzed for early apoptosis (annexin-V$^+$, LD dye$^-$, lower right quadrant) and cell death (annexin-V$^+$, LD dye$^+$, upper right quadrant) (Figure 12 F and G). Viable cells are shown in the lower left quadrant of Figure 12 F and G.

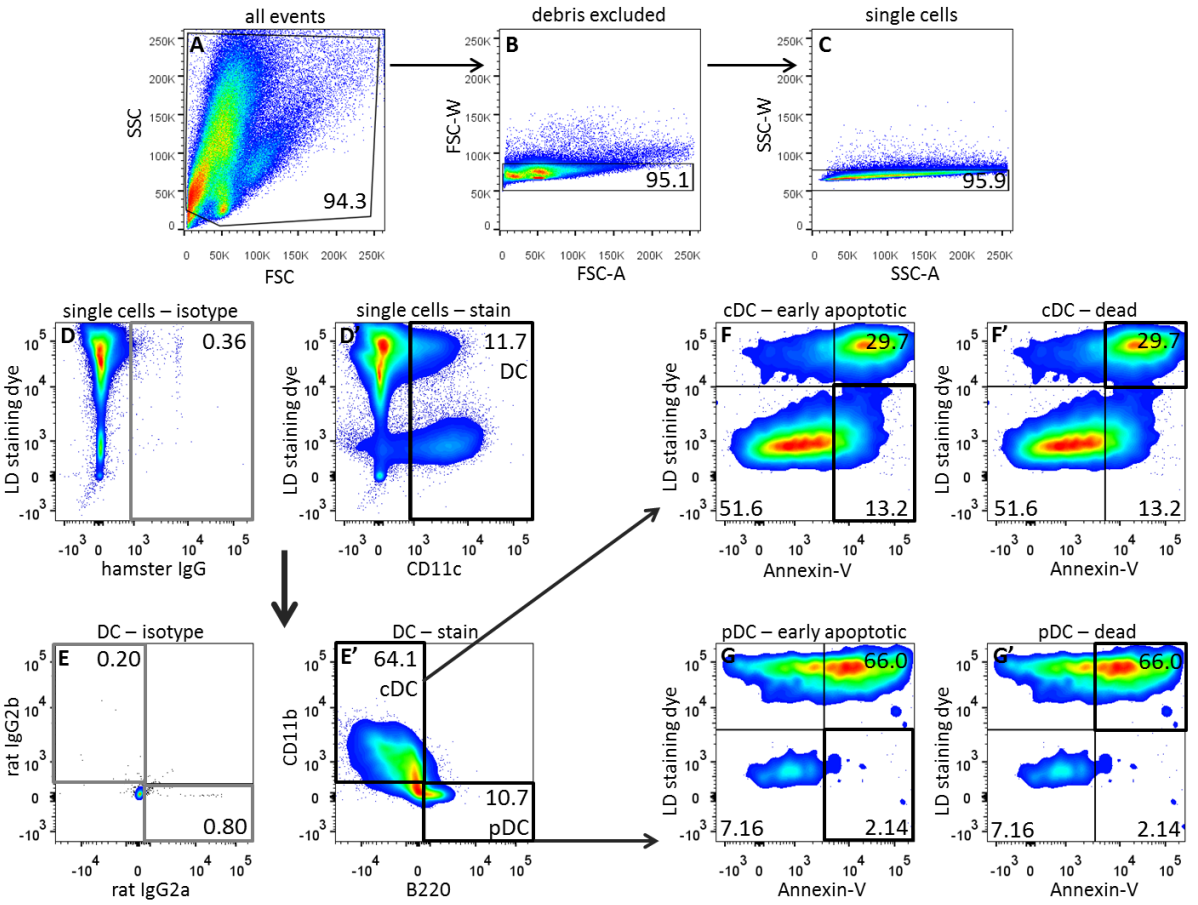

Figure 12: Gating strategy for the detection of early apoptosis in pDC and cDC
A: exclusion of cell debris, **B:** gating FSC-A against FSC-W to exclude doublets, **C:** gating SSC-A against SSC-W to exclude doublets, **D/D':** gating for CD11c$^+$ cells representing DC, gate is set according to the isotype (D), **E/E':** gating for CD11b$^+$ events representing cDC and B220$^+$ events representing pDC, gates are set according to the particular isotypes (E), **F:** gating for annexin-V$^+$ and LD dye$^-$ cDC to determine the percentage of early apoptotic cDC, **F':** gating for annexin-V$^+$ and LD dye$^+$ cDC to determine the percentage of dead cDC, **G:** gating for annexin-V$^+$ and LD dye$^-$ pDC to determine the percentage of early apoptotic pDC. **G':** gating for annexin-V$^+$ and LD dye$^+$ pDC to determine the percentage of dead pDC. Viable cells are represented by annexin-V$^-$ and LD dye$^-$ events (lower left quadrant of F and G). CpG-ODN-stimulated cells are shown as example.

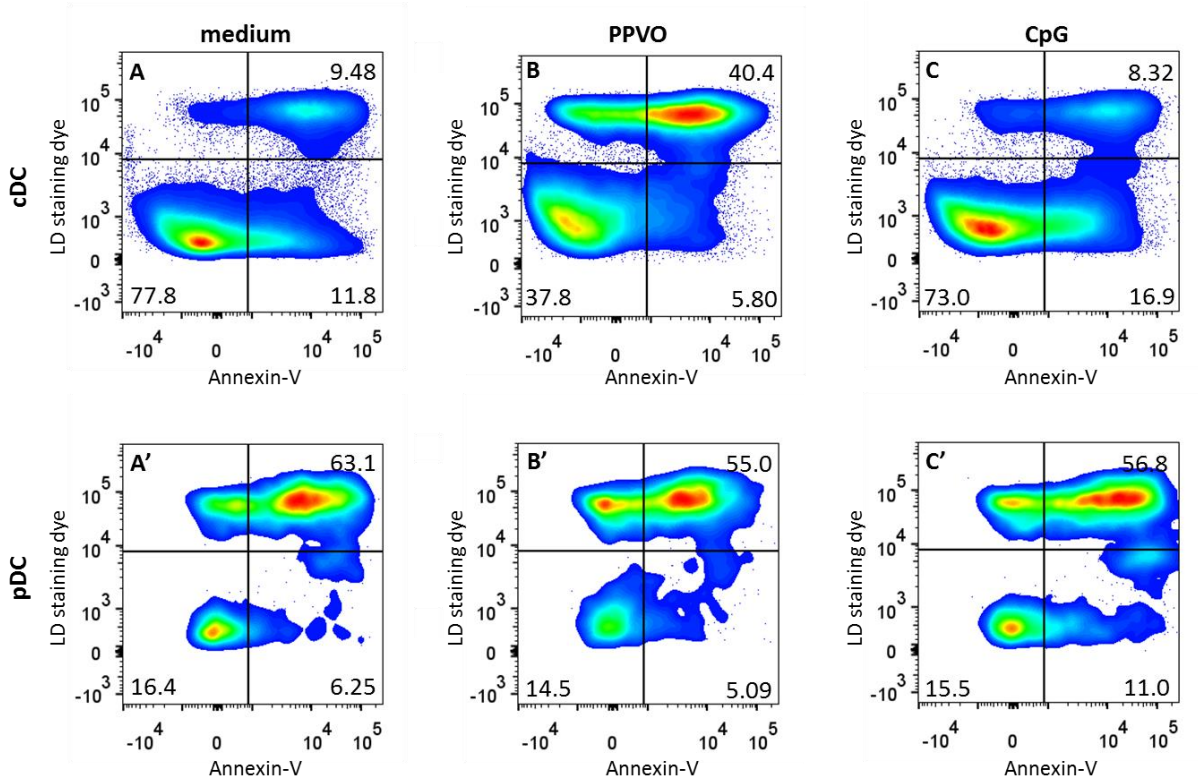

Figure 13: Viability of pDC and cDC in response to PPVO
FLDC were infected with PPVO at MOI 10, stimulated with CpG-ODN or left untreated (medium). 24 hours post-infection, cells were stained with annexin-V and LD dye and analyzed by flow cytometry. Plots were gated on cDC ($CD11b^+$) and pDC ($B220^+$) following doublet exclusion. Viability of cDC in response to PPVO (**B**), CpG-ODN (**C**) or in medium control (**A**).

PPVO infection led to a severe reduction of cDC viability within 24 hours (Figure 13) indicating a strong cytotoxic effect. In contrast to that, the pDC viability, which was already very low in medium, was not affected by PPVO infection. Stimulation with CpG-ODN had no effect on the viability of cDC or pDC (Figure 13 D).

Variable results were obtained for the analysis of early apoptosis in two different experiments. Further studies are required to determine whether PPVO induces apoptosis in DC or elicits anti-apoptotic effects. However, my data demonstrate that PPVO induces cell death in cDC but not in pDC.

Keratinocytes were gated the same way as FLDC. Cell debris and doublets were excluded and cells were analyzed for early apoptosis and cell death (Figure 14) and compared to FLDC.

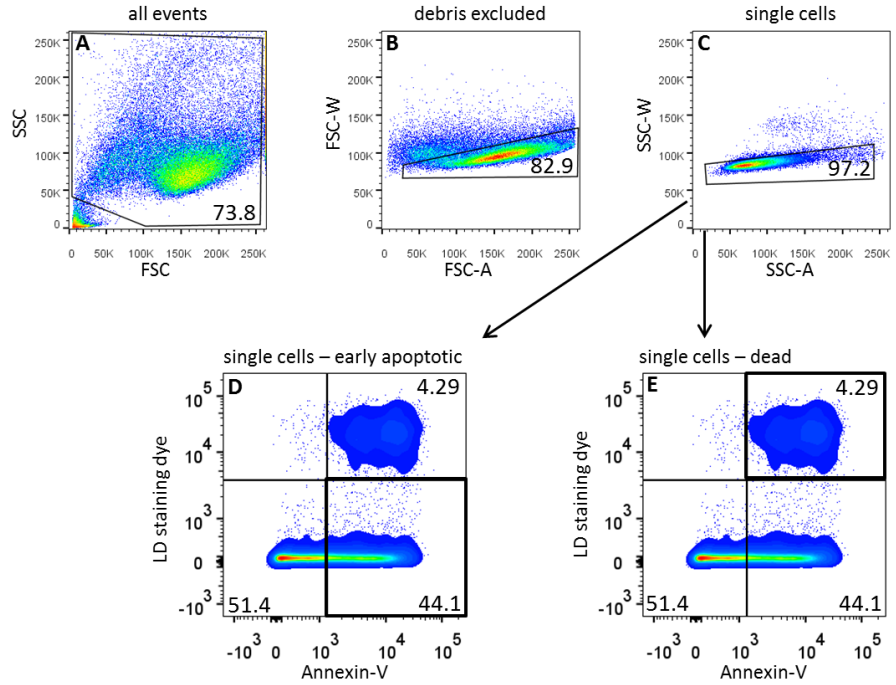

Figure 14: Gating strategy for the detection of apoptotic rates in keratinocytes
A: cell debris was excluded, **B:** gating FSC-A against FSC-W to exclude doublets, **C:** gating SSC-A against SSC-W to exclude doublets, **D:** gating for annexin-V^+ and LD dye^- cells to determine the percentage of cells being in an early apoptotic state, **E:** gating for annexin-V^+ and LD dye^+ cells to determine the percentage of dead cells. Viable cells are represented by annexin-V^- and LD dye^- events (lower left quadrant of D and E). IFN-γ-stimulated cells are shown as example.

After 24 hours, infection with PPVO (MOI 1) and stimulation with IL-17A/TNF-α supported the viability of keratinocytes, whereas IFN-γ and PPVO at MOI 10 had no effect (Figure 15 D). 72 hours post-stimulation, PPVO at MOI 1 still supported keratinocyte viability, whereas MOI 10 again had no effect. Interestingly, IL-17A/TNF-α stimulation led to a severe reduction in viability, indicating an early protective effect that is gone after 72 hours. In line with these data, PPVO stimulation at MOI 1 reduced the proportion of early apoptotic cells 24 hours (Figure 15 E) and 72 hours (Figure 15 E') post-infection. At the higher dose (MOI 10), PPVO infection resulted in cell death after 72 hours (Figure 15 D'). These data indicate that low MOIs of PPVO elicit anti-apoptotic effects in murine keratinocytes, whereas higher doses of PPVO lead to cell death.

Taken together, these data show that PPVO strongly affects the viability of DC and to a much lower degree of keratinocytes indicating that the degree of cell activation induced by PPVO infection correlates with cytotoxicity.

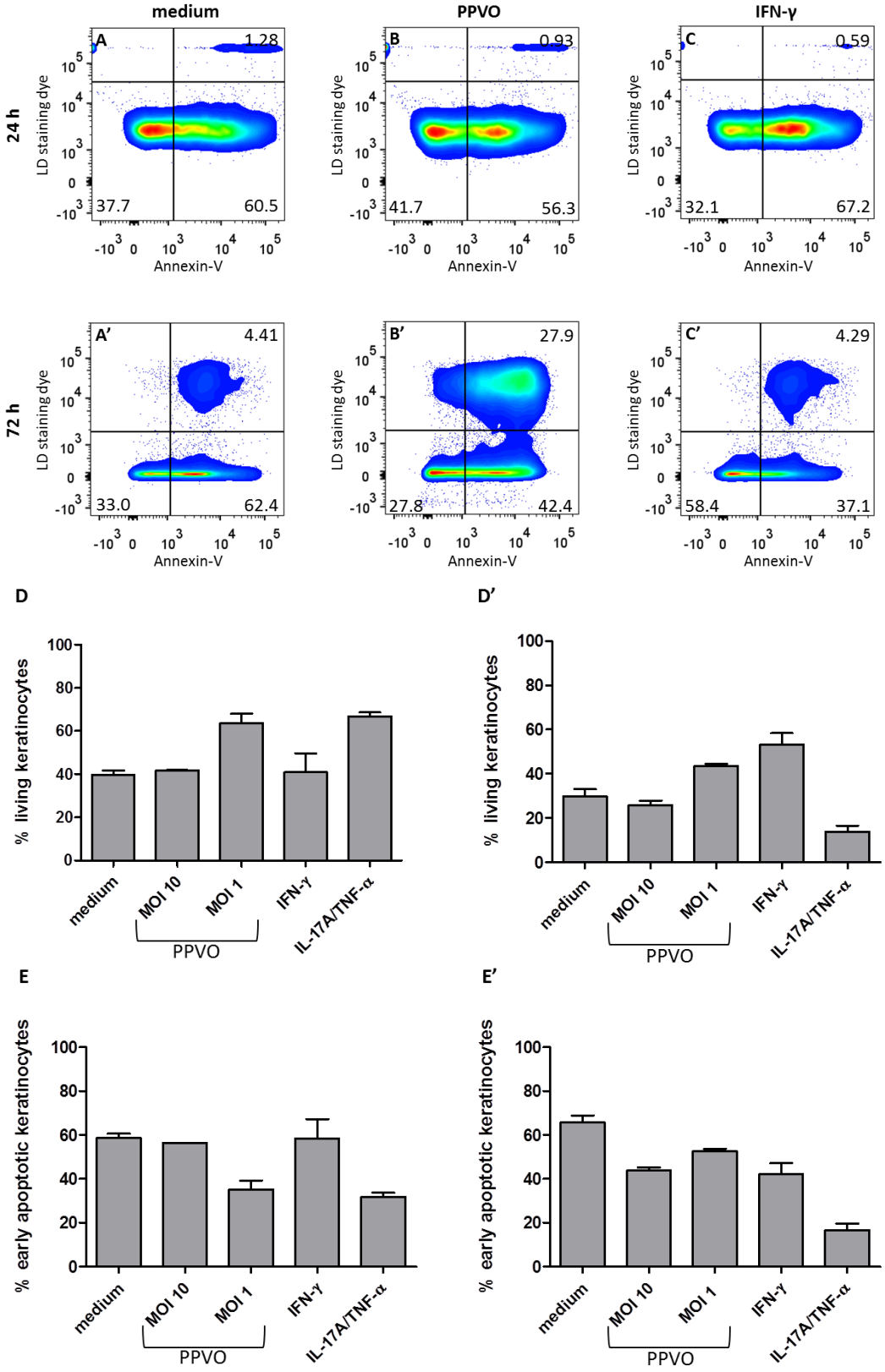

Figure 15: Viability of keratinocytes in response to PPVO
Cells were infected with PPVO at MOI 10 (**B**) or 1, stimulated with IFN-γ or IL-17A/TNF-α or left untreated (medium). 24 (**A-C**) or 72 hours (**A'-C'**) post-infection, cells were stained with annexin-V and LD dye and analyzed by flow cytometry. Plots were gated on single cells. **D/D':** percentage of living keratinocytes in response to PPVO or cytokine stimulation, **E/E':** percentage of early apoptotic keratinocytes in response to PPVO or cytokine stimulation. One representative of two independent experiments is shown.

4.3 Detection of PPVO in FLDC and keratinocytes

The second approach to explain the different cytokine and surface marker responses to PPVO infection by keratinocytes and FLDC, was to investigate potential differences in the magnitude of PPVO uptake. Therefore, a staining protocol was established and fluorescence microscopy was done to gain insight into the extra- or intracellular localization of PPVO. Infected FLDC and keratinocytes were stained for the PPVO envelope protein F1L and analyzed by laser scanning microscopy (Zeiss LSM 780).

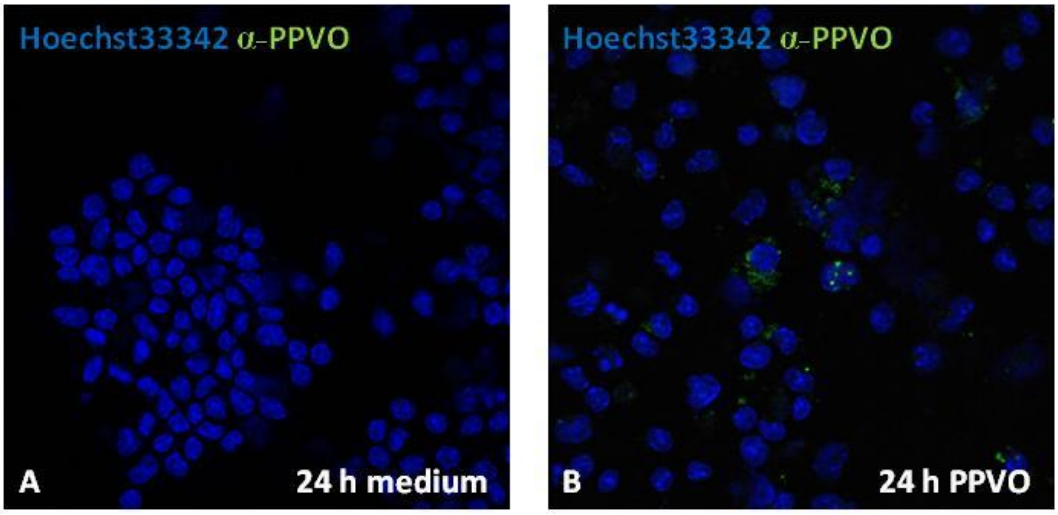

Figure 16: Detection of PPVO in FLDC
FLDC were infected with PPVO at MOI 10. 24 hours post-infection, nuclei were stained with Hoechst33342 (blue) and the PPVO envelope protein F1L was stained with a Cy2-labeled donkey anti-mouse IgG conjugate (green). Unstimulated cells stained with the primary and secondary antibody conjugate are shown as negative control (**A**) in comparison to PPVO-infected cells (**B**). Magnification: 63x.

Some single positive cells showing weak signals for PPVO fluorescence in close vicinity to the Hoechst-stained nuclei were observed in PPVO-infected FLDC indicating an uptake of virus particles (Figure 16). These results confirm previous electron microscopy studies of PPVO uptake by FLDC (Siegemund *et al.*, 2009). In comparison to unstimulated cells, the total cell number of infected FLDC was decreased (data not shown) consistent with the reduction of viability shown above (see Figure 13). No difference in cell morphology was observed upon PPVO infection. In the medium control, incubated with the same primary antibody and secondary antibody conjugate, no fluorescent staining was observed, demonstrating that no nonspecific binding of the antibodies has occurred.

Localization studies of PPVO were already done in primary ovine fibroblasts. By confocal microscopy, a punctual distribution of the virus in the cytoplasm was observed (Diel *et al.*,

2011). The same could be seen in experiments with murine keratinocytes that were analyzed during this study. Keratinocytes showed stronger signals for PPVO-associated fluorescence than FLDC. 24 hours post-infection, a punctate distribution of PPVO around the nucleus was observed indicating the uptake of PPVO in membrane compartments (e.g. Golgi or endoplasmic reticulum) (Figure 17 B and C). After 72 hours, PPVO (MOI 10) could be detected scattered in the cytosol (Figure 17 C'). The total cell numbers of infected keratinocytes strongly increased dependent on the applied MOI and slight differences in cell morphology were observed. Cells infected with PPVO (MOI 10) were roundly shaped after 72 hours indicating a cytopathic effect of PPVO. Uninfected keratinocytes, stained with the primary and secondary antibody conjugate, showed no fluorescence signals, confirming that no nonspecific binding of the used antibodies has occurred.

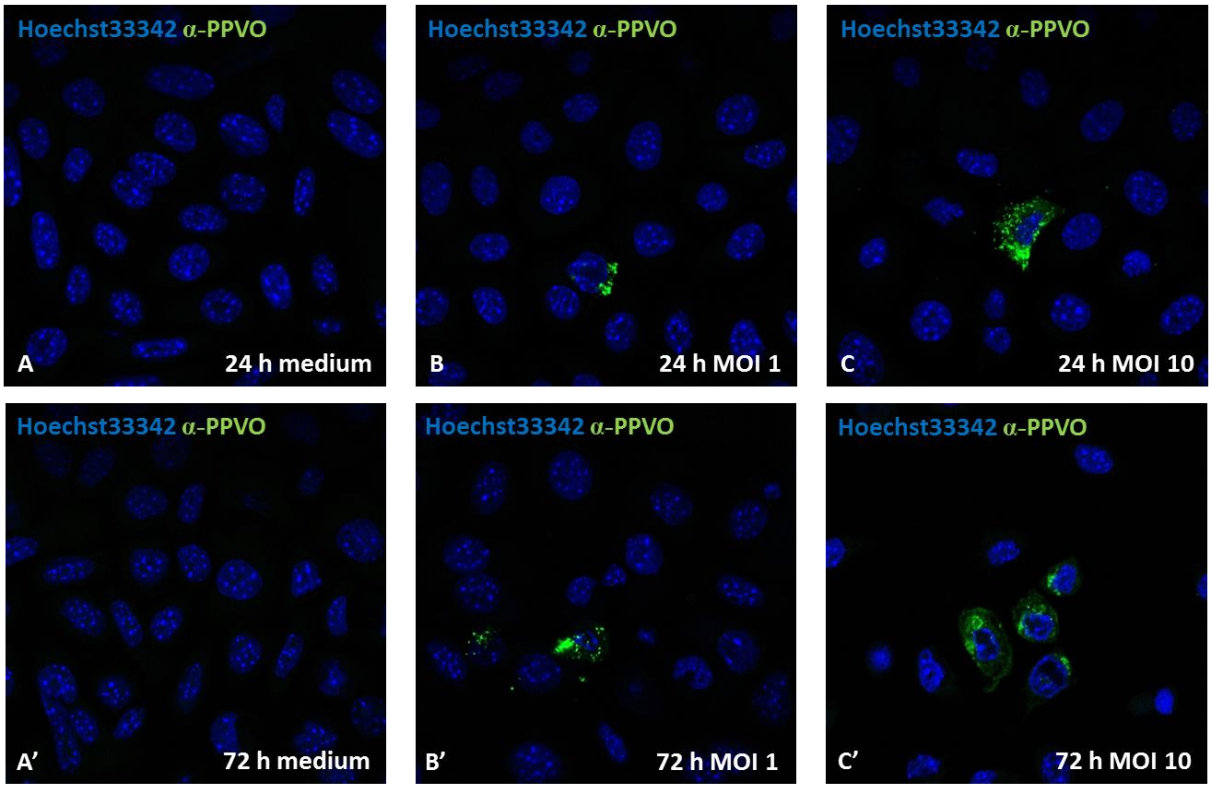

Figure 17: PPVO uptake in keratinocytes
Cells were infected with PPVO at MOI 10 (**C**) or 1 (**B**). 24 (**A-C**) or 72 hours (**A'-C'**) post-infection, nuclei were stained with Hoechst33342 (blue) and the PPVO envelope protein F1L was stained with a Cy2-labeled donkey anti-mouse IgG conjugate (green). Unstimulated cells stained with the primary and secondary antibody conjugate as well are shown as negative control (**A**) in comparison to PPVO-infected cells (**B, C**). Magnification: 63x.

To quantify the number of cells associated with PPVO signals (i.e. possibly infected cells), stained cells were counted and divided by the total cell number to obtain the percentage of positive cells (Figure 18). After 24 hours, the percentage of possibly infected FLDC was

increased in comparison to keratinocytes. The percentage of infected keratinocytes was dependent on the PPVO dose and the incubation time (Figure 18 B). The signals in FLDC were weak and it could not be distinguished clearly whether PPVO is taken up by the cells or is associated with the cell membrane. In contrast to that, PPVO was clearly detectable intracellular in keratinocytes. On a per cell basis keratinocytes seemed to be more efficient in PPVO uptake than FLDC (Figure 16 andFigure 17). By immunofluorescence studies, no significant differences in PPVO uptake were detected to provide an explanation for the differences in cytokine and surface marker response of FLDC and keratinocytes. To reveal possible variations in the intracellular distribution and to confirm the uptake of PPVO by FLDC, further studies are necessary.

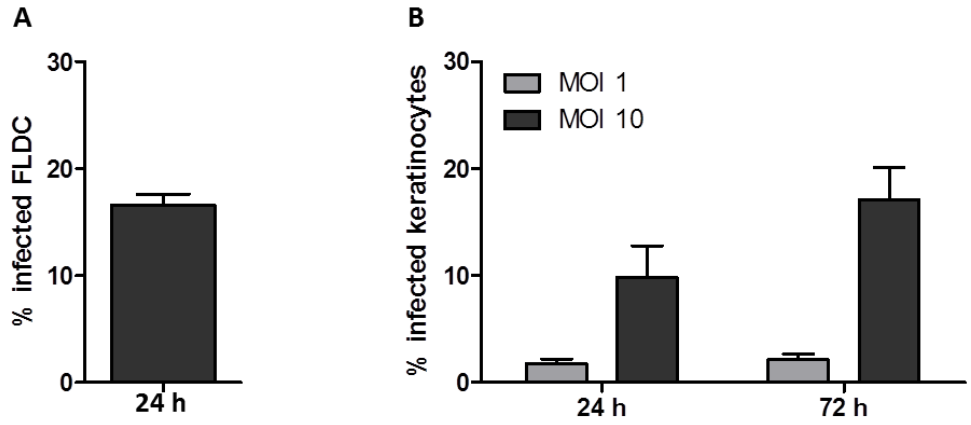

Figure 18: Percentage of FLDC (A) and keratinocytes (B) associated with fluorescently labeled PPVO
FLDC and keratinocytes were infected with PPVO at MOI 10 (FLDC, keratinocytes) or 1 (keratinocytes). 24 (A, B left columns) or 72 hours (B right columns) post-infection, cells were fixed and stained with an antibody against the PPVO envelope protein F1L. Stainings were analyzed by fluorescence microscopy (magnification: 20x). Five microscopic fields were taken from each sample. The cells associated with PPVO were considered "infected" based on the immunofluorescent signals located in close vicinity to the Hoechst-stained nuclei and divided by the total number of cells on each photograph. Graphs show pooled data of two independent experiments.

5. Discussion

PPVO causes contagious ecthyma (orf, scabby mouth, contagious pustular dermatitis), a debilitating disease characterized by the formation of localized skin lesions. Among cutaneous cell populations, keratinocytes are supposed to be the target cells for PPVO replication in permissive hosts (Dal Pozzo *et al.,* 2005). The interactions of keratinocytes with PPVO are poorly understood. In non-permissive hosts, PPVO has been successfully used for the development of recombinant vector vaccines due to its immunostimulatory capacity (Fischer *et al.,* 2003). Dendritic cells (DC) as professional antigen-presenting cells are among the first sentinels against invading pathogens such as PPVO. DC phagocytose pathogens and process and present antigens on their surface to activate naïve T cells (Banchereau *et al.,* 2000). The major aim of my study was to compare the response of keratinocytes and DC to PPVO contact.

The results of my study show that PPVO induces a strong reaction in DC rather than keratinocytes. DC secrete TNF-α (Figure 1) upon PPVO stimulation indicating the occurrence of a PPVO-triggered inflammatory response (Beutler and Cerami, 1989). Additionally, DC produced the pro-inflammatory IL-12p40, IL-6 and type I and III interferons but not IL-1β in response to PPVO (data not shown). PPVO also induced the expression of MHC-II and the co-stimulatory molecule CD86 on DC (Figure 6). These results demonstrate that PPVO activates DC. Thus, the present data are in line with previous reports of DC activation by PPVO (Siegemund *et al.,* 2009).

In contrast to DC, murine keratinocytes produced TNF-α constitutively but did not upregulate TNF-α production in response to PPVO (Figure 2). Keratinocytes did not produce the pro-inflammatory cytokines IL-6, IL-12p40 and type I and III interferons observed by DC. However, keratinocytes produced IL-1β upon PPVO contact, indicating that keratinocytes are able to sense and react to PPVO. The activation state of keratinocytes was also characterized by the expression of surface molecules. Human keratinocytes constitutively express MHC-I (Basham *et al.,* 1984). Moreover, murine keratinocytes were shown to increase the expression of MHC-II under inflammatory conditions (Gaspari and Katz, 1988). In this study, no induction of MHC-I or MHC-II expression upon infection with PPVO was observed on murine keratinocytes (Figure 8 and 9), indicating that no PPVO-triggered inflammation occurred. Moreover, PPVO did not induce the expression of ICAM-1, or PD-L1, surface proteins involved in inflammation and immune regulation, respectively (Wawryk *et al.,* 1989; Groeger *et al.,* 2011). Stimulation of keratinocytes with IFN-γ induced the expression of ICAM-1 (Figure 10) and PD-L1 (Figure 11), excluding an intrinsic defect of murine

keratinocytes to respond to stimulation. Taken together, the data of cytokine production and surface marker expression indicate that PPVO strongly stimulates DC but has much weaker if any stimulatory effects on murine keratinocytes.

One possible explanation for the different responses to PPVO infection could be differences in its cytopathic effect on DC and keratinocytes. Therefore, the viability of DC and keratinocytes was analyzed and the proportion of early apoptotic and dead (i.e. late apoptotic and necrotic) cells upon stimulation and PPVO infection was determined by flow cytometry. PPVO stimulation for 24 hours profoundly reduced the viability of cDC but not pDC (Figure 13). Former studies reported that PPVO induces apoptosis in monocytes and macrophages (Garrido-Farina *et al.,* 2008; Kruse and Weber, 2001). However, in those studies cells were stained with annexin-V only and no counterstain with a viability dye was performed, so that no distinction between early apoptotic and necrotic cells was technically possible. Another study reported anti-apoptotic effects of PPVO on infected HeLa cells and identified the apoptosis inhibitor ORFV125 (Westphal *et al.,* 2007). Thus, it is conceivable that it depends on the infected cell type, whether PPVO induces apoptosis or exerts anti-apoptotic effects. In the FLDC experiments, variable data for apoptosis were revealed in two approaches. Therefore, no final conclusion can be drawn until further experiments are done. Nevertheless, my data support the notion of cell type specific responses to PPVO, as PPVO dramatically reduced the viability of cDC but had no effect on the viability of pDC (Figure 13) and keratinocytes (Figure 15). Whereas the viability of DC is reduced after 24 hours post-infection with PPVO, the percentage of dead keratinocytes is not affected at this time point. At 72 hours post-infection, the proportion of dead keratinocytes is strongly increased in response to PPVO (MOI 10) (Figure 15 B'). These findings were also observed in ovine organotypic cultures infected with PPVO. Here, a cytopathic effect characterized by balloon degeneration of epidermal cells was observed 48 hours post-infection (Scagliarini *et al.,* 2005). PPVO replication is promoted in proliferating cells. This could be the reason for the late occurrence of the PPVO-mediated cytotoxic effect on the slowly proliferating keratinocytes.

In summary, the analysis of cell death and viability revealed fundamental differences between FLDC and keratinocytes with FLDC being more susceptible to the cytotoxic effect of PPVO. One would expect that an increase in cell death would lead to a decrease in the ability to get activated which could not be observed in the case of FLDC. Instead, my findings demonstrate a correlation of cell death and the ability to get stimulated. Possibly, the increase in cell death

is not directly mediated by PPVO but a consequence of activation. Though, this was not observed upon CpG-ODN treatment where the activation state of FLDC is more pronounced. Concerning early apoptosis, the data for keratinocytes do not suggest the induction of apoptosis by PPVO. For FLDC further studies are necessary as the obtained results during this study were not clear-cut. Possibly, other methods such as TUNEL or caspase assays could reveal clearer results as they are known to have a higher sensitivity than annexin-V/7-AAD staining. These techniques would also enable the fixation of the cells which could increase the reproducibility of the results.

The second approach to explain the different outcome of stimulating DC and keratinocytes was to identify cell type-dependent differences in virus uptake. To my knowledge, no studies exist about the intracellular localization of PPVO in murine keratinocytes. In the present study, I show that PPVO can infect both cell types, DC and keratinocytes (Figure 18). The fluorescently labeled PPVO envelope protein F1L was detected in close proximity to the Hoechst-stained nuclei in DC indicating an uptake of PPVO. This confirms previous findings demonstrating by electron microscopy that PPVO can be taken up by DC and is localized in endosomal compartments as well as in the cytoplasm (Siegemund *et al.*, 2009). Due to the small cell size and the low amount of cytoplasm within these cells it is hard to determine whether PPVO is localized intracellular or only associated with the cell surface. The large poxvirus particles can enter many cell types via macro-pinocytosis (Mercer and Helenius, 2008). To confirm the uptake of PPVO by immunofluorescence and to gain insight into the intracellular distribution of the virus, further experiments are necessary. A possible approach would be to treat unfixed cells with trypsin to rule out the extracellular localization of PPVO. In case of extracellular PPVO, the fluorescent signals would disappear. It was reported that PPVO can be detected in a punctate distribution in the cytoplasm in epithelial ovine turbinate cells (Diel *et al.*, 2011). Indeed, I found PPVO in the cytoplasm of keratinocytes. To clearly identify the intracellular localization of PPVO in keratinocytes and to gain insight into its infection pathway, further immunofluorescence studies are necessary. Co-stainings of PPVO and membrane compartments (e.g. endosomes, Golgi apparatus) would be an interesting attempt for the future.

The uptake of PPVO into murine keratinocytes was dose-dependent and increased over time (Figure 18 B). In comparison to DC, the amount of PPVO per cell is higher in keratinocytes. This could be due to the larger size of keratinocytes. However, the percentage of infected cells is higher in DC than in keratinocytes at 24 hours. Thus, DC seem to be more susceptible to

PPVO infection. This observation fits to the stronger cytotoxic effect of PPVO on DC and to their activation state.

The major aim of my study was to investigate the different behavior of DC and keratinocytes in response to PPVO contact. By analyzing the production of cytokines and the expression of activation markers, it was revealed that DC are strongly activated by PPVO (e.g. upregulation of MHC-II, production of pro-inflammatory cytokines), whereas the production of cytokines as well as the expression of activation markers (e.g. ICAM-1) by keratinocytes was not affected by PPVO uptake. PPVO caused a severe reduction of the viability of cDC but had a much weaker cytotoxic effect on keratinocytes. The uptake of PPVO occurred earlier in DC, but the ingested particle amount seemed to be higher in keratinocytes.
In summary, the responses to PPVO infection were fundamentally different between the two investigated cell types. Possibly, the two cell types express a different set of receptors leading to different signaling pathways triggered by PPVO. DC are professional antigen-presenting cells, keratinocytes are non-professional (Kotzerke *et al.*, 2013). This could also contribute to the responses of these cells to PPVO infection. As professional antigen-presenting cells, DC get activated and have the ability to activate other cells (e.g. T cells) without the aid of interactions with other cells. Keratinocytes could need the support of other cells or at least signals mediated by other cells to get activated. IL-1 is an initiation signal for keratinocyte activation (Freedberg *et al.*, 2001). Langerhans cells (LC), one DC subtype of the skin, are known to be producers of IL-1 (Schreiber *et al.*, 1992). This suggests that keratinocytes might need the interaction with cells such as LC to be successfully activated. Keratinocytes were shown to produce IFN-α and IL-18 upon activation. Both cytokines act on LC as activation signals and induce a Th1 immune response (Hari *et al.*, 2010). Therefore, the further analysis of keratinocytes in co-culture with LC would be a promising approach.

References

Banchereau, J.; Briere, F.; Caux, C.; Davoust, J.; Lebecque, S.; Liu, Y. J. et al. (2000): Immunobiology of dendritic cells. In *Annual Review of Immunology* 18, pp. 767–811.

Basham, T. Y.; Nickoloff, B. J.; Merigan, T. C.; Morhenn, V. B. (1984): Recombinant gamma interferon induces HLA-DR expression on cultured human keratinocytes. In *The Journal of Investigative Dermatology* 83 (2), pp. 88–90.

Beutler, B.; Cerami, A. (1989): The biology of cachectin/TNF--a primary mediator of the host response. In *Annual Review of Immunology* 7, pp. 625–655.

Dal Pozzo, F.; Andrei, G.; Holy, A.; Van Den Oord, J.; Scagliarini, A.; Clercq, E. de; Snoeck, R. (2005): Activities of Acyclic Nucleoside Phosphonates against Orf Virus in Human and Ovine Cell Monolayers and Organotypic Ovine Raft Cultures. In *Antimicrobial Agents and Chemotherapy* 49 (12), pp. 4843–4852.

Diel, D. G.; Luo, S.; Delhon, G.; Peng, Y.; Flores, E. F.; Rock, D. L. (2011): Orf virus ORFV121 encodes a novel inhibitor of NF-kappaB that contributes to virus virulence. In *Journal of Virology* 85 (5), pp. 2037–2049.

Fan, L.; Busser, B. W.; Lifsted, T. Q.; Oukka, M.; Lo, D.; Laufer, T. M. (2003): Antigen presentation by keratinocytes directs autoimmune skin disease. In *Proceedings of the National Academy of Sciences of the United States of America* 100 (6), pp. 3386–3391.

Fischer, T.; Planz, O.; Stitz, L.; Rziha, H.-J. (2003): Novel recombinant parapoxvirus vectors induce protective humoral and cellular immunity against lethal herpesvirus challenge infection in mice. In *Journal of Virology* 77 (17), pp. 9312–9323.

Freedberg, I. M.; Tomic-Canic, M.; Komine, M.; Blumenberg, M. (2001): Keratins and the keratinocyte activation cycle. In *The Journal of Investigative Dermatology* 116 (5), pp. 633–640.

Friebe, A.; Siegling, A.; Friederichs, S.; Volk, H.-D.; Weber, O. (2004): Immunomodulatory effects of inactivated parapoxvirus ovis (ORF virus) on human peripheral immune cells: induction of cytokine secretion in monocytes and Th1-like cells. In *Journal of Virology* 78 (17), pp. 9400–9411.

Garrido-Farina, G. I.; Cornejo-Cortes, M. A.; Martinez-Rodriguez, A.; Reyes-Esparza, J.; Alba-Hurtado, F.; Tortora-Perez, J. (2008): A study of the process of apoptosis in animals infected with the contagious ecthyma virus. In *Veterinary Microbiology* 129 (1-2), pp. 28–39.

Gaspari, A. A.; Katz, S. I. (1988): Induction and functional characterization of class II MHC (Ia) antigens on murine keratinocytes. In *Journal of Immunology* 140 (9), pp. 2956–2963.

Groeger, S.; Domann, E.; Gonzales, J. R.; Chakraborty, T.; Meyle, J. (2011): B7-H1 and B7-DC receptors of oral squamous carcinoma cells are upregulated by Porphyromonas gingivalis. In *Immunobiology* 216 (12), pp. 1302–1310.

Haig, D. M. (2006): Orf virus infection and host immunity. In *Current Opinion in Infectious Diseases* 19 (2), pp. 127–131.

Haig, D. M.; McInnes, C. J.; Deane, D. L.; Reid, H. W.; Mercer, A. A. (1997): The immune and inflammatory response to orf virus. In *Comparative Immunology, Microbiology and Infectious Diseases* 20 (3), pp. 197–204.

Haig, D. M.; Mercer, A. A. (1998): Ovine diseases. Orf. In *Veterinary Research* 29 (3-4), pp. 311–326.

Halliday, K. E.; McKenzie, R. C.; and Norval, M. (1997): Expression of interleukin-10 mRNA in herpes simplex virus-infected keratinocytes in vivo and in vitro. In *Biochemical Society Transactions* 25, p. 282.

Hari, A.; Flach, T. L.; Shi, Y.; Mydlarski, P. R. (2010): Toll-like receptors: role in dermatological disease. In *Mediators of Inflammation* 2010, p. 437246.

Kawai, T.; Akira, S. (2006): Innate immune recognition of viral infection. In *Nature Immunology* 7 (2), pp. 131–137.

Kotzerke, K.; Mempel, M.; Aung, T.; Wulf, G. G.; Urlaub, H.; Wenzel, D. et al. (2013): Immunostimulatory activity of murine keratinocyte-derived exosomes. In *Experimental Dermatology* 22 (10), pp. 650–655.

Kruse, N.; Weber, O. (2001): Selective induction of apoptosis in antigen-presenting cells in mice by Parapoxvirus ovis. In *Journal of Virology* 75 (10), pp. 4699–4704.

Kupper, T. S. (1990): The activated keratinocyte: a model for inducible cytokine production by non-bone marrow-derived cells in cutaneous inflammatory and immune responses. In *The Journal of Investigative Dermatology* 94 (6 Suppl), pp. 146S-150S.

Liu, L.; Xu, Z.; Fuhlbrigge, R. C.; Pena-Cruz, V.; Lieberman, J.; Kupper, T. S. (2005): Vaccinia virus induces strong immunoregulatory cytokine production in healthy human epidermal keratinocytes: a novel strategy for immune evasion. In *Journal of Virology* 79 (12), pp. 7363–7370.

Matsunaga, T.; Katayama, I.; Yokozeki, H.; Nishioka, K. (1996): ICAM-1 expression on keratinocytes in mechanically-injured skin of a patient with atopic dermatitis. In *Journal of Dermatological Science* 12 (3), pp. 219–226.

McKeever, D. J.; Jenkinson, D. M.; Hutchison, G.; Reid, H. W. (1988): Studies of the pathogenesis of orf virus infection in sheep. In *Journal of Comparative Pathology* 99 (3), pp. 317–328.

Mercer, J.; Helenius, A. (2008): Vaccinia virus uses macropinocytosis and apoptotic mimicry to enter host cells. In *Science* 320 (5875), pp. 531–535.

Payne, L. G.; Norrby, E. (1978): Adsorption and penetration of enveloped and naked vaccinia virus particles. In *Journal of Virology* 27 (1), pp. 19–27.

Peña-Cruz, V.; McDonough, S. M.; Diaz-Griffero, F.; Crum, C. P.; Carrasco, R. D.; Freeman, G. J. (2010): PD-1 on immature and PD-1 ligands on migratory human Langerhans cells regulate antigen-presenting cell activity. In *The Journal of Investigative Dermatology* 130 (9), pp. 2222–2230.

Pospischil, A.; Bachmann, P. A. (1980): Nuclear changes in cells infected with parapoxviruses stomatitis papulosa and orf: an in vivo and in vitro ultrastructural study. In *The Journal of General Virology* 47 (1), pp. 113–121.

Scagliarini, A.; Dal Pozzo, F.; Gallina, L.; Guercio, A.; Clercq, E. de; Snoeck, R.; Andrei, G. (2005): Ovine skin organotypic cultures applied to the ex vivo study of orf virus infection. In *Veterinary Research Communications* 29, pp. 245–247.

Scagliarini, A.; Gallina, L.; Dal Pozzo, F.; Battilani, M.; Ciulli, S.; Prosperi, S. (2004): Heparin binding activity of orf virus F1L protein. In *Virus Research* 105 (2), pp. 107–112.

Schreiber, S.; Kilgus, O.; Payer, E.; Kutil, R.; Elbe, A.; Mueller, C.; Stingl, G. (1992): Cytokine pattern of Langerhans cells isolated from murine epidermal cell cultures. In *Journal of Immunology* 149 (11), pp. 3524–3534.

Siegemund, S.; Hartl, A.; Buttlar, H. von; Dautel, F.; Raue, R.; Freudenberg, M. A. et al. (2009): Conventional bone marrow-derived dendritic cells contribute to toll-like receptor-independent production of alpha/beta interferon in response to inactivated parapoxvirus ovis. In *Journal of Virology* 83 (18), pp. 9411–9422.

Smith, G. L.; Vanderplasschen, A.; Law, M. (2002): The formation and function of extracellular enveloped vaccinia virus. In *The Journal of General Virology* 83 (Pt 12), pp. 2915–2931.

Steinman, R. M.; Inaba, K. (1999): Myeloid dendritic cells. In *Journal of Leukocyte Biology* 66 (2), pp. 205–208.

Tolonen, N.; Doglio, L.; Schleich, S.; Krijnse Locker, J. (2001): Vaccinia virus DNA replication occurs in endoplasmic reticulum-enclosed cytoplasmic mini-nuclei. In *Molecular Biology of the Cell* 12 (7), pp. 2031–2046.

Vanderplasschen, A.; Hollinshead, M.; Smith, G. L. (1998): Intracellular and extracellular vaccinia virions enter cells by different mechanisms. In *The Journal of General Virology* 79 (Pt 4), pp. 877–887.

Wawryk, S. O.; Novotny, J. R.; Wicks, I. P.; Wilkinson, D.; Maher, D.; Salvaris, E. et al. (1989): The Role of the LFA-1/ICAM-1 Interaction in Human Leukocyte Homing and Adhesion. In *Immunological Reviews* 108 (1), pp. 135–161.

Westphal, D.; Ledgerwood, E. C.; Hibma, M. H.; Fleming, S. B.; Whelan, E. M.; Mercer, A. A. (2007): A novel Bcl-2-like inhibitor of apoptosis is encoded by the parapoxvirus ORF virus. In *Journal of Virology* 81 (13), pp. 7178–7188.

Wick, M. J. (2007): Monocyte and dendritic cell recruitment and activation during oral Salmonella infection. In *Immunology Letters* 112 (2), pp. 68–74.

Wise, L. M.; Inder, M. K.; Real, N. C.; Stuart, G. S.; Fleming, S. B.; Mercer, A. A. (2012): The vascular endothelial growth factor (VEGF)-E encoded by orf virus regulates keratinocyte

proliferation and migration and promotes epidermal regeneration. In *Cellular Microbiology* 14 (9), pp. 1376–1390.

Wittek, R.; Kuenzle, C. C.; Wyler, R. (1979): High C + G content in parapoxvirus DNA. In *The Journal of General Virology* 43 (1), pp. 231–234.

Danksagung

Zu allererst möchte ich mich bei Prof. Dr. Gottfried Alber dafür bedanken, dass er mich in seiner Arbeitsgruppe aufgenommen und mir die Möglichkeit gegeben hat, meine Masterarbeit in seinem Team anzufertigen. Vielen Dank für die stetige Unterstützung und die Bereitschaft, jederzeit alle Fragen zu beantworten und eventuell auftretende Probleme zu diskutieren. Danke auch für die Begutachtung meiner Arbeit und die zahlreichen Ratschläge, die zum Gelingen dieser beigetragen haben.

Bei Prof. Dr. Thomas Magin bedanke ich mich für die wiederholte, freundliche Übernahme des Gutachtens an der Fakultät für Biowissenschaften, Pharmazie und Psychologie. Für die unkomplizierte Abwicklung und die Unterstützung bin ich sehr dankbar. Zudem bedanke ich mich für die Bereitstellung der Keratinozyten-Zelllinie. Hierbei geht ein besonderer Dank an Gabi Baumbach für die Einführung in die Keratinozyten-Kultur und die Vorbereitung des Mediums.

Ein besonderer Dank gilt außerdem Dr. Heiner von Buttlar, der mich in meiner Anfangszeit betreut hat und mir mit seinem umfangreichen Wissen über Viren, ihre Abwehr und die Techniken, mit denen man diese untersuchen kann, eine große Hilfe war.

Bei Dr. Sabine Siegemund bedanke ich mich für die intensive Betreuung meiner Arbeit, ihre Geduld bei der Beantwortung aller auftretenden Fragen und ihr stetiges Vertrauen in meine Fähigkeiten, vor allem dann, wenn es mir selbst fehlte. Nicht zuletzt danke ich ihr, wie auch Prof. Dr. Mathias Büttner, für das kritische Lesen meiner Arbeit.

Ein ganz besonderer Dank geht an die Kollegen vom Institut für Immunologie, Doris Bismarck, Bianca Schulze, Maria Eschke, Dr. Daniel Piehler, Laura Heyen, Anett Grohs, Dr. Martina Protschka, Dr. Uwe Müller und Silke Lehnert, die mich herzlich in ihren Kreis aufgenommen haben und mir von Anfang an mit Rat und Tat zur Seite standen. Danke für die wunderbare Atmosphäre, auch abseits des Laboralltages.

Meinen Freunden danke ich dafür, dass ich immer auf sie zählen kann, sie mich jederzeit unterstützen, mich wenn nötig motivieren und aufbauen und dafür sorgen, dass ich auch mal

abschalte und das Leben neben der Arbeit nicht vergesse – allen voran Bea und Sandra. Ihr seid die Besten!

Der größte Dank aber gilt meinen Eltern, auf deren Unterstützung ich mich immer verlassen kann, die immer hinter mir stehen und mir in allen Lebenslagen eine großartige Hilfe sind.